The Biological Bulletin, December 2021, volume 241, number 3: 000–000. https://doi.org/10.1086/716552

Progress Toward Complete Life Cycle Culturing of the Endangered Sunflower Star, *Pycnopodia helianthoides*

J. HODIN*, A. PEARSON-LUND†, F. P. ANTEAU, P. KITAEFF, AND S. CEFALU

Friday Harbor Laboratories, University of Washington, Friday Harbor, Washington 98250

Abstract. Until recently, the sunflower star, *Pycnopodia helianthoides*, was a dominant and common predator in a wide variety of benthic habitats in the NE Pacific. Then, in 2013, its populations began to plummet across its entire range as a result of the spread of a phenomenon known as sea star wasting disease, or sea star wasting. Although dozens of sea star species were impacted by this wasting event, *P. helianthoides* seems to have suffered the greatest losses and is now listed by the International Union for the Conservation of Nature as the first critically endangered sea star. In order to learn more about the life history of this endangered predator and to explore the potential for its restoration, we have initiated a captive rearing program to attempt complete life cycle (egg-to-egg) culture for *P. helianthoides*. We report our observations on holding and distinguishing individual adults, reproductive seasonality, larval development, inducers of settlement, and early juvenile growth and feeding. These efforts will promote and help guide conservation interventions to protect remaining populations of this species in the wild and facilitate its ultimate return.

Introduction

In 2013, a mass mortality of asteroids caused by sea star wasting disease, or sea star wasting (SSW), was first observed in the NE Pacific. By 2016, every known species of asteroid in the region was impacted, from obligatorily intertidal taxa to deep-sea specialists. Perhaps the species that was most severely affected by SSW was the sunflower star, *Pycnopodia helianthoides* (Brandt, 1835). Populations across its entire range, from the Alaskan Aleutian Islands to Baja California, were reduced, in some cases quite severely (Harvell *et al.*, 2019). Indeed, this formerly common intertidal and subtidal species may have been extirpated from the southern third of its range (Gravem, 2020). In December 2020, *P. helianthoides* was listed as critically endangered by the International Union for Conservation of Nature (IUCN, 2020; see also Gravem *et al.*, 2020), the first endangered species listing for any sea star.

Among its unique features, *P. helianthoides* has numerous arms (up to 24 when full grown) and is the largest known asteroid, with an arm tip-to-arm tip diameter of up to 65 cm (Feder, 1980). It is also a notably mobile sea star, traveling speeds of up to 2 m min^{-1} under duress (N. McDaniel, Subsea Enterprises, pers. comm.). These features, along with its generalist diet, make it a potent subtidal predator of a wide range of sessile and sedentary invertebrate taxa (Feder, 1980; Sloan, 1980; Shivji *et al.*, 1983), often eliciting dramatic escape responses in potential prey species. For example, a brief contact with a sunflower star causes the typically sedentary California sea cucumber, *Apostichopus californicus*, to immediately undertake an undulating, swimming, and crawling response that lasts for over 30 min (Margolin, 1976).

Sunflower stars are major generalist predators in a variety of ecosystems in the NE Pacific, including soft subtidal areas, rocky intertidal shoals, and kelp forests (Shivji *et al.*, 1983). One notable type of prey of sunflower stars is sea urchins of the genus *Strongylocentrotus* (Dayton, 1975; Feder, 1980; Duggins, 1983). In recent years, coincident with the enormous die-offs of sunflower stars from SSW, there has been a tremendous increase in populations of the purple urchin, *Strongylocentrotus purpuratus*, in waters off of central and northern California (Rogers-Bennett and Catton, 2019). Purple urchins are, in turn, dominant grazers of the kelp forest-forming bull kelp, *Nereocystis luetkeana*, a species that has seen massive

Received 13 February 2021; Accepted 14 July 2021; Published online XX Month 2021.

* To whom correspondence should be addressed. Email: hodin@uw.edu.

† Present address: Deeley Research Centre, BC Cancer, Victoria, British Columbia V8R 6V5, Canada.

Abbreviations: 1-MA, 1-methyladenine; dpf, days post-fertilization; FHL, Friday Harbor Laboratories; GVBD, germinal vesicle breakdown; MFSW, ≤1-μm filtered seawater; pf, post-fertilization; SSW, sea star wasting.

Online enhancements: supplemental tables and figures, data supplement.

declines in the past decade (Rogers-Bennett and Catton, 2019; Finger *et al.*, 2021). Together, these coincident population shifts have raised the possibility that the disappearance of sunflower stars as a result of SSW (and the absence of other predators, such as otters; Kenyon, 1969) has released purple urchins from predatory pressure, leading to or exacerbating the kelp population crashes (Burt *et al.*, 2018). This recent transition in parts of the NE Pacific from a kelp-dominant to an urchin-dominant benthos is a probable instance of an ecological phase shift: a non-continuous alteration in the characteristics of an ecosystem from one stable state to an alternate stable state (Done, 1992).

The restoration of an extirpated species, such as *P. helianthoides*, might help restore the ecological state that preceded the phase shift. In the case of the NE Pacific kelp forest ecosystem, recovery of ancestrally dominant sea otter and sunflower star populations might reinstitute control of urchins, thus allowing for natural or human-assisted kelp recovery. This led us to undertake captive rearing of *P. helianthoides*, with dual goals of investigating basic questions involving sunflower star life history and ecological functions and sensitivities, and also exploring the long-term possibility of reintroductions to the wild.

Sea stars have been a widely studied taxon for embryonic and larval development, as well as larval ecology (reviewed in Chia and Walker, 1991; Metaxas, 2013; Hodin *et al.*, 2019). A broad taxonomic array of species, including sunflower stars (Greer, 1962), have been reared from egg through metamorphosis into newly settled juveniles. By contrast, few publications have documented successful attempts to rear sea stars beyond their early post-settlement stages as they grow into sub-adults. Indeed, we are aware of only one study documenting successful lab rearing of a forcipulate sea star (Forcipulatida, a diverse order of stars that includes *P. helianthoides*) with a feeding larva (planktotrophy): the New Zealand reef star, *Stichaster australis* (Barker, 1979).

Settlement in most planktotrophic sea stars occurs at a diameter of about 0.5 mm (Emlet *et al.*, 1987), which means that the juveniles of most taxa grow more than 2 orders of magnitude before attaining adult size. Clearly, the juveniles and adults are feeding on quite different things. In the case of *S. australis*, the juveniles graze on coralline algae and then switch to carnivory later in life (Barker, 1979), a phenomenon described for other sea star taxa as well (Martinez *et al.*, 2017). Much less is known for species in which the post-settlement stages are carnivores.

Here we report on our initial progress toward realizing full life cycle (egg-to-egg) rearing of *P. helianthoides* in captivity. We detail observations on collecting, holding, and distinguishing individual adults, as well as spawning, fertilization, larval development, settlement, and early juvenile growth and survival in small-scale culture. Although, as previously stated, larval development in sea stars is well described (McEdward and Miner, 2001), the endangered status of sunflower stars merits detailed descriptions of their larval stages, and in particular their approach to settlement and the transformation itself. We present our findings in the hope that they will spark further interest and efforts in captive breeding of this iconic species, one that has a potentially pivotal function in maintaining healthy coastal ecosystems in the NE Pacific.

Materials and Methods

Collecting, feeding, holding, and distinguishing adults

From March through September 2019, in and around San Juan Island, Washington, we collected 35 adult *Pycnopodia helianthoides* (Brandt, 1835) (>20 cm arm tip-to-arm tip diameter; henceforth, diameter), intertidally and off of dock pilings by hand and subtidally by scuba from 3- to 20-m depth. The director of Friday Harbor Laboratories (FHL) approved collections of sunflower stars in the San Juan Archipelago under the auspices of state statute (House Bill 68, R.C.W.28.77.230, 1969 Revision R.C.W.28B.20.320), with FHL as the managing agency.

From nine adult *P. helianthoides* collected on a single dive near Juneau on July 22, 2019 (S. Tamone, University of Alaska–Southeast, Alaska Department of Fish and Game permit CF-19-031), we obtained gametes for fertilizations as described below and in *Results*. For reproductive assessments, colleagues at the Washington State Department of Fish and Wildlife collected *P. helianthoides* adults for us on two occasions from a sizable population in Hood Canal, Washington: August 2019 (12 adults on a single dive) and January 2020 (6 adults on a single dive). We also assessed reproductive status in one individual collected by colleagues in August 2020, which eventually succumbed to wasting.

After collection, we transported adults in coolers filled with freshly collected seawater in 1 hour or less to FHL, where we maintained adults in 1-m-deep, partially covered outdoor opaque flow-through natural seawater aquaria under high flow. We fed adults a diet consisting mainly of mussels (*Mytilus trossulus*) every other day. A standard feeding consisted of 1 large mussel (~70–120 g wet weight) or 2 medium mussels (~30–60 g wet weight). Water temperature in the aquaria where we housed adults varied from ~9 °C to 14 °C throughout the year. At the time of this writing (July 2021), we have held 28 stars continually for 24 months with no mortality or signs of wasting.

The color patterns in *P. helianthoides* are remarkably variable (Fig. 1; Fig. S1, data supplement, available online), to the point where we can distinguish all 28 of these captive stars by appearance for tracking purposes. In addition to color and patterns, we also note the position of regenerating arms with respect to the madreporite as a distinguishing feature (Fig. S1F, data supplement, available online) and measured them over time in all of our captive stars to assess regeneration rates. Additional details on specific characters that we use to positively and consistently identify individual stars can be found

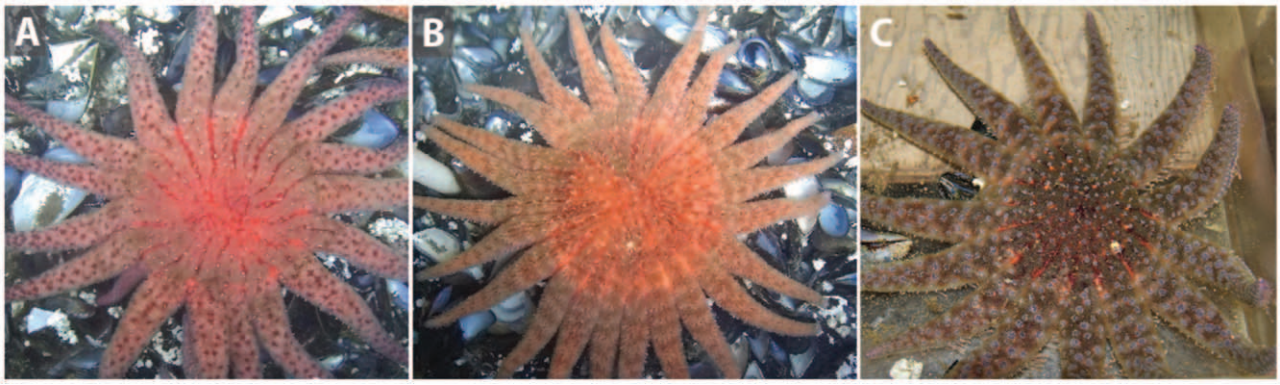

Figure 1. Color variation in *Pycnopodia helianthoides*. We used features including disk and arm color, position of regenerating arms (A), spine color and prominence (A, C), and arm stripe patterns (B, C) to positively identify individual stars in our colony and track them over time.

in Figure S1. Further notes on collecting and holding adults can be found in the data supplement (available online).

Assessing reproductive status, obtaining gametes, maturation, and fertilization

Like most asteroids, *P. helianthoides* is dioecious; males and females are not distinguishable by known external features. We assessed the reproductive status of our captive adults by 1 of 5 methods: (1) injection with 1 mL of the spawning and maturation hormone 1-methyladenine (1-MA) per 100 mL of sea star volume (Strathmann, 1987; Adams *et al.*, 2019); (2) making an incision of a small (1 cm × 1 cm) flap in the aboral epidermis in the proximal portion of an arm; (3) arm amputation; (4) gonad examination in stars that had self-autotomized or otherwise lost an arm (*e.g.*, as a consequence of SSW) or otherwise suffered an aboral wound; or (5) direct observation of spontaneous spawning.

Adult *P. helianthoides* increased activity for 30–45 min following 1-MA injection (assessment method 1); but very few spawned, despite repeated attempts at different times of year. In only one case did a female spawn by this method, releasing a limited quantity of eggs, though they were fertilizable. We observed no disease or lethality following any injection.

See the data supplement (available online) for more details on our spawning attempts with 1-MA injection, as well as our notes on assessment method 2, aboral incisions, which we do not recommend, and assessment method 3, arm autotomy by dissection, which has been our preferred method and has been followed in all cases by full recovery of the stars and regeneration of the missing arm.

We observed spontaneous spawnings on several occasions in captive stars: May 2020 and March, April, and May 2021. Males spawned in all four of these cases, and females spawned in two of them; we recovered fertilized eggs from both of the latter events (see Table 1). Therefore, with careful observation of held stars, spontaneous spawnings could be a viable method of starting larval cultures without further interventions.

Oocytes are often oblong in shape; our reported diameters are averages of the longest diameter and the diameter perpendicular to that, both passing approximately through the centroid (n = 10–20 oocytes measured per individual). See the data supplement (available online) for notes on assessing the viability and maturity of dissected male and female gonadal tissue, including slide preparation techniques for measuring oocyte diameters, as well as final maturation of oocytes with *in vitro* 1-MA treatments. See also Strathmann (1987) and Adams *et al.* (2019) for more detailed methods.

We accomplished successful *in vitro* fertilizations on four occasions, using dissected gonad from stars in which arms had been amputated: in July 2019 deriving from Alaskan (AK) *P. helianthoides* parents, and in November 2019, April 2020, and January 2021 deriving from Washington (WA) parents. We reared larvae from all of these fertilizations except April 2020, in which the fertilizations were for reproductive assessment only. For the AK stars, the day after amputation, our colleagues in Juneau sent us gonad by overnight mail; we set up fertilizations upon arrival the following day (thus, 2 days after amputation). For the WA stars, we set up the fertilizations the same day as the amputations. Table 1 summarizes the details of all successful fertilizations, including two deriving from events of spontaneous spawning in captive stars.

Embryogenesis and larval development

At 10–11 °C, early bipinnaria larvae are ready to feed at 5 days post-fertilization (dpf). We cultured them initially at ~1 larva mL^{-1} and fed them a mixture of the live microalgae *Dunaliella tertiolecta* and *Rhodomonas* sp. at 3000 cells mL^{-1} and 2500 cells mL^{-1}, respectively. We cultured larvae in glass jars, using a motor-driven stirring apparatus (see M. Strathmann, 1987; R. Strathmann, 2014). Every 2 days, we changed 95% of the culture water by either gentle reverse or forward filtration (see Hodin *et al.*, 2019) and then fed the larvae as above.

Table 1

Details of seven successful fertilizations, 2019–2021, using stars collected in Alaska (AK) and Washington (WA)

Collection dates and general location	Adults amputated	Adults with mature gonad	Fertilization date	Fate of offspring
Auke Bay, SE AK, July 23–24, 2019	4M, 3F	4M, 1F	July 26, 2019	Raised through metamorphosis in quarantine; used in juvenile feeding experiment
San Juan Island, WA, July–August 2019	2M, 4F	2M, 2F	November 5, 2019	Raised through metamorphosis; juveniles still being reared
San Juan Island, WA, May–August 2019	3M, 2F	2M, 2F	April 24, 2020	Fertilization confirmed; not reared
San Juan Island, WA, July–August 2019	n/a (spontaneous spawning)	? (cloudy water indicated that spawning had occurred but was not itself observed)	May 22, 2020	Larvae present; not reared
San Juan Island, WA, July–August 2019	4M, 2F	4M, 2F	January 20, 2021	Larvae and juveniles currently being reared
San Juan Island, WA, July–August 2019	n/a (spontaneous spawning)	At least 2M, 2F	March 18–19, 2021	Embryos recovered; not reared
San Juan Island, WA, July–August 2019	n/a (1-MA injections)	3M, 1F	April 4, 2021	Embryos recovered; not reared

1-MA, 1-methyladenine; AK, Alaska; F, female; M, male; n/a, XXX; WA, Washington.

At ~25 dpf, the left and right coelomic sacs had fused anteriorly (*i.e.*, anterior to the mouth) and were within ~10 μm of fusing posteriorly (*i.e.*, posterior to the stomach). At this point, we began to thin the cultures stepwise over 2 successive water changes: initially to ~0.5 larva mL^{-1}, and 2 days later to ~0.25 larva mL^{-1}. We continued to culture them at this latter density through settlement. Juvenile skeleton first appeared in the rudiments of larvae at ~27 dpf. See *Results* for further details on structures that we use to stage these late-stage larvae as they approach competence.

Settlement and completion of metamorphosis

See the data supplement (available online) for our definitions of metamorphosis and settlement. Starting on ~50 dpf, larvae will settle spontaneously (namely, in the absence of a specific cue) on the sides of the culture vessels. Larval attachment with the brachiolar apparatus of *P. helianthoides* is remarkably firm, presumably employing a secreted cement previously described in other asteroids (Barker, 1978). As such, settling larvae are resistant to mechanical dislodgement even from a directed jet of seawater from a squirt bottle. Thus, we recommend scrubbing the walls of the vessels thoroughly at each water change to remove the biofilm to which the competent larvae are apparently attracted. Doing so greatly limits the aforementioned spontaneous settlement, allowing the investigator to elicit settlement in the containers in which the juveniles will be reared.

Despite the rigid adhesion to the surface exhibited by settled larvae, they can be manipulated by gently tapping the side of the juvenile body with a glass Pasteur or plastic transfer pipette. Doing so generally induces the juvenile to transiently release its attachment, at which point it can be sucked up into the pipette and quickly moved to a new location if desired (quick movement is necessary to prevent the juvenile from adhering to the inside of the pipette). This entire process is best done with care under a binocular microscope, so as not to harm the juvenile in the process.

Competent brachiolaria larvae have well-developed opaque helmets (defined further in *Results*) of juvenile skeleton at the posterior margin, clearly visible in a binocular dissecting scope. We employ half-pint (0.24-L) wide-mouth glass canning jars for settlement assays involving exposure to natural settlement inducers (biofilms, coralline algae) and in some cases following turbulence exposures, as described below. These jars can be immersed in tanks to accumulate biofilm, contain sufficient volume (0.2 L) of seawater to allow larvae to swim freely and at a comparable larval density to their larval cultures, and can be viewed easily in a binocular dissecting scope.

To test for settlement induction following biofilm exposures, we first immersed replicate jars in flow-through aquaria at FHL containing adults of *P. helianthoides*, purple urchins (*Strongylocentrotus purpuratus*), mussels (*Mytilus trossulus*), or mixed invertebrates (a display tank) or with no macroinvertebrates present (general biofilm). We accumulated biofilm for 7 d unless otherwise noted and then maintained those jars at 11 °C with ≤1-μm filtered seawater (MFSW) exchanges every 2 d until conducting settlement assays. We used the same style of replicate jars for settlement assays with the coralline alga *Calliarthron tuberculosum*, at an exposure density of 0.65 g of algal fronds in 100 mL of settlement water.

To investigate the modulation of larval settlement responses by turbulence, we employed both a quantifiable method and a more qualitative method of generating turbulence and compared them (along with a control) in a single experiment. We began by selecting seemingly competent WA-derived larvae at 113 dpf into beakers containing 100 mL of MFSW. We selected 20–25 larvae into each of 12 beakers, after which we randomly assigned the beakers to 1 of 3 treatments: (1) the quantifiable turbulence method, (2) the qualitative turbulence method, or (3) unexposed controls. We exposed larvae from each replicate run to turbulence or control conditions for 3 min, after which we poured all recovered larvae from a run into glass finger bowls for observations of larvae swimming *versus* those on the bottom (*i.e.*, contacting the walls of the bowl) and then assessed settlement over 24 h by immediately transferring all of the larvae to a jar—1 jar per run—containing biofilm exposed to adult *P. helianthoides* for 5 d (and then maintained for 5 additional days before the experiment; see above).

For the quantifiable turbulence method, we employed a Taylor-Couette cell (Taylor, 1923; Karp-Boss *et al.*, 1996; Denny *et al.*, 2002), a standard device used to produce and study both laminar and turbulent flows in the laboratory. See the data supplement (available online) for details on this device and specific exposures used.

Following the 3-min exposures in the device in 125 mL, we gently poured the larvae into a 1-L beaker containing ~100 mL of MFSW and then rinsed the device 2 times with MFSW to recover any adhered larvae, concentrated the larvae by gentle reverse filtration, and then proceeded with settlement observations as above. We rinsed the device with distilled water between runs to ensure that no larvae remained before starting the next exposure.

For the qualitative method of generating turbulence, we similarly poured larvae from the selection beakers into 125 mL total MFSW in 250-mL Erlenmeyer flasks, covered the tops with parafilm, and then exposed them to 3 min of oscillatory shaking (~240 repetitions min^{-1}) to simulate turbulence, keeping the flask vertical the entire time. After exposure, we poured the entire contents of the flask into a glass finger bowl and rinsed the beaker one time with MFSW to recover any adhered larvae. Controls were treated identically to the shaken larvae, except that we left the flasks undisturbed for the 3-min duration.

Culturing juveniles post-settlement

In our initial efforts to culture the post-settlement stages, the juveniles experienced high mortality. We attribute this mortality to a combination of the following causes: (1) physical damage, (2) contaminants, (3) closed culture, and (4) cannibalism. See the data supplement (available online) for more detailed notes on these four causes of juvenile mortality. Another possibility, but one that we were unable to evaluate, is that some of the juveniles succumbed to SSW.

Our subsequent, more successful efforts at juvenile rearing (*i.e.*, with higher juvenile survival and growth rates) involved culturing juveniles in flow-through cages (food-grade plastic tubs with windows cut in the side covered by 100–200-μm Nitex mesh; Genesee Scientific, San Diego, CA). We initiated this design in March 2019 (with 0–2-mo post-settlement juveniles), using recirculating ~10-gal MFSW tanks, with water changes in the tanks every 4 d. We used 30 gal h^{-1} fountain pumps (Danner Manufacturing, Islandia, NY) to enhance circulation around the cages and fed water from additional pumps through seawater manifolds to deliver positive water flow through each tank.

In November 2019 (with 7–9-mo post-settlement juveniles), we improved this design by using continuously flowing natural seawater filtered down to a nominal 1 μm before entering the holding tank in which our cages were situated. Juvenile survival stabilized under these conditions, and growth rates increased (see *Results*).

Feeding. The greatest challenge in culturing *P. helianthoides* was identifying suitable food for the earliest juvenile stages. We tried a range of possible food sources for the early juveniles, including natural multispecies biofilms, cultivated biofilms of benthic diatoms (B2042 *Nitzschia frustulum* and B2046 *Navicula incerta*; UTEX, Austin, TX), epiphytes and epizoites on coralline algae, small pieces of kelp, newly settled echinoid juveniles, a commercial fish diet (Otohime larval feed B1, 200–360-μm size range; Pentair Aquatic Eco-Systems, Apopka, FL), and cultivated bivalve juveniles (the cockle *Laevicardium elatum* [from the Puget Sound Restoration Fund] and the Manila clam *Venerupis philippinarum* and the Pacific oyster *Miyagi oyster* [both from Taylor Shellfish Farms, Shelton, WA]). Either we offered *P. helianthoides* juveniles intact juvenile bivalves or we crushed the juvenile bivalve shells with forceps to give young *P. helianthoides* juveniles access to tissues. We provide feeding observations in *Results*.

Beginning about 35 d after settlement, we conducted a feeding experiment with AK-derived juveniles, using separated halves of plastic tea infusers (~200-μm mesh; Upton Tea Imports, Holliston, MA; henceforth, filter baskets). Once the filter baskets had cured for several weeks in natural seawater containers to generate a biofilm, we placed two juveniles into each basket and set them in a shallow aquarium with rapidly recirculating flow (95 gal h^{-1}) and with the upper half of the basket above the water level. We then haphazardly assigned baskets to one of three test treatment groups or a control. In the treatment groups, juveniles were fed (*a*) 1–2 crushed juvenile cockles *Laevicardium elatum*, (*b*) 10 early post-settlement (~300-μm test diameter) *Dendraster excentricus* juveniles, or (c) 10 grains of Otohime larval feed B1 (200–360-μm size range; Pentair Aquatic Eco-Systems). The control juveniles were not fed (aside from the biofilm already present). We positioned the filter baskets in a table of recirculating UV-treated MFSW such that water could not flow over the tops of the baskets.

During the feeding experiment, we examined the juveniles every 2 d to watch for changes in gross morphology (normal or shriveled), coloration (colored or pale), and activity levels (active or sluggish) as indicators of overall health. We replaced food on an as-needed basis, as available food ran low, or as we observed fouling of uneaten food. We shifted the basket positions in the water table every 2 d to promote similar flow conditions for each basket. We ran the experiment for 50 d in December 2019 through January 2020.

Transport of different life stages

See the data supplement (available online) for detailed methods on transporting gametes, larvae juveniles, and adult *P. helianthoides*.

Microscopy and measurements

We observed, measured, and photographed live embryos and larvae, gently immobilized under cover glass raised with modeling clay (see Strathmann, 2014), at 40× to 400× magnification, using a variety of compound microscopes. We visualized larval and incipient juvenile skeleton by using cross-polarized light and made measurements by using calibrated ocular micrometers or from calibrated micrographs.

We measured and photographed juveniles *in situ* by using binocular microscopes furnished with an ocular micrometer and reflected (episcopic) light. At larger sizes (>1 cm), we also used calipers for size measurements.

Statistics

We conducted all statistical analyses with R (ver. 3.5.2; R Core Team, 2017). For the majority of our settlement experiments and for the feeding experiment, we used a logistic (generalized linear) mixed-effects model, employing the lme4 and emmeans packages (Bates *et al.*, 2015; Lenth, 2018), to analyze data due to the binomial nature of our response variables (*e.g.*, larvae settled or knocked down). In our tests, we treated each replicate exposure (jar, *etc.*) of a group of larvae as a random intercept. In two experiments (the temporal comparison of settlement on *P. helianthoides vs.* general biofilm; and in the analysis of juvenile size in the feeding experiment) we conducted an ANOVA. These two types of analyses can be distinguished in *Results* by the types of statistics shown: we report *Z*-statistics for the logistic mixed-effects models and *F*-statistics for ANOVAs. All of our reported *P*-values are after employing Bonferroni corrections for multiple comparisons.

Results

Adult arm regeneration rates

For the purpose of collecting gonad, we amputated 1 arm in 22 of our captive stars over the course of 16 mo. In 12 of these 22 stars, we amputated an additional arm after a minimum 6-mo recovery period. All amputated arms subsequently began to regenerate (see, *e.g.*, Fig. S1F, data supplement, available online), with an average rate of regeneration of 0.11 ± 0.05 (SD) mm d^{-1}, or 4.0 ± 1.8 cm yr^{-1}. The average arm length in the captive stars in November 2020 was 12.4 ± 1.6 (SD) cm. Therefore, based on our observed regeneration rates, we predicted that it would take between 2.7 and 4.2 yr (95% confidence interval [CI]) for the sunflower stars to fully regenerate their lost or amputated arms. Individual regeneration rates were not strongly correlated with differences in body size ($r = 0.144$). Note that we were not attempting to feed the sea stars *ad libitum* during this study, for fear of overfeeding them. Thus, it is possible that our data represent underestimates of maximum potential regeneration rates.

Oocyte sizes, reproductive maturity, and fertilizations

We measured oocyte diameters in amputated stars as well as several others that lost an arm for another reason, including SSW. Table S1 (data supplement, available online) lists oocyte sizes for each of these stars and, if treated with the maturation hormone 1-MA, whether the oocytes underwent germinal vesicle breakdown (GVBD) and were ultimately fertilized; Figure 2 plots these data over time for the WA stars. Individuals in which the largest oocytes were ~150 μm in diameter or less did not undergo GVBD and did not fertilize ($n = 8$). Based on the results listed in Figure 2 and Table S1, we suggest that the reproductive season for females of this species in WA begins in November–January and ends in April–May. Mature and fertilizable oocytes from *P. helianthoides* in SE Alaska were isolated by a colleague in July 2019. It is likely that the reproductive season for females is later in this northern part of the species range. Egg sizes across all individuals that we examined ranged from 155 to 170 μm (Table S1).

Table S1 lists the results for several females that we amputated twice, with a minimum of 6 mo between amputations. Two of those females did not have mature oocytes on their first amputations (late 2019) but did have mature oocytes 16–18 mo later (early 2021), indicating that they completed their reproductive cycle in captivity.

In males, by contrast, we did not observe strong evidence for reproductive seasonality. We successfully recovered testes containing mature sperm from the amputated arms of males throughout the year (data not shown). Furthermore, we observed a testis completely devoid of sperm on only one occasion, yet we also had a successful spawning of a male sunflower star by the standard technique of 1-MA injection that same month, May 2019. Note that we did not attempt to measure gonad size as a proxy for reproductive cycling because recovering the entire gonad during amputation would have involved increased stress to the adults.

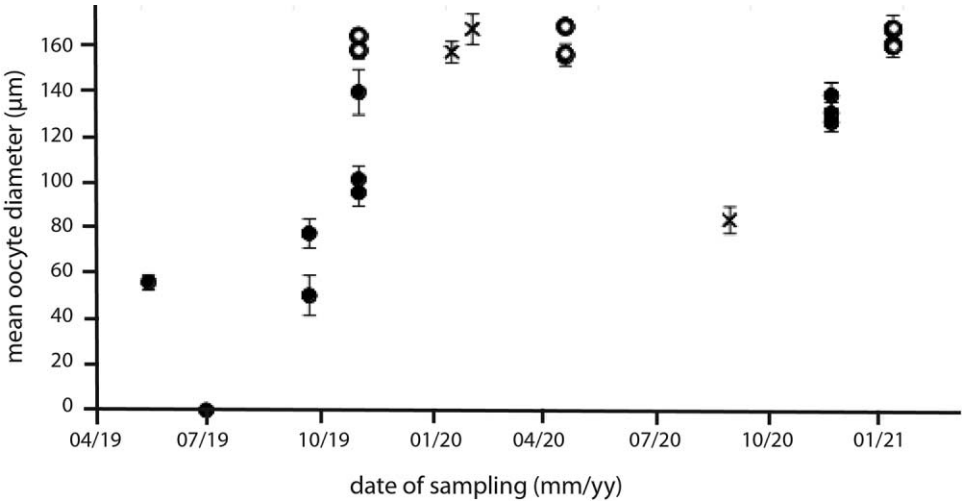

Figure 2. Oocyte sizes in Washington-collected *Pycnopodia helianthoides*. Filled circles indicate oocytes that, when treated with 1-methyladenine (1-MA), did not undergo germinal vesicle breakdown (GVBD) and become fertilizable, that is, immature oocytes. Open circles indicate oocytes that underwent GVBD and became fertilizable after treatment with 1-MA, that is, mature oocytes. X indicates data from preserved ovaries, not treated with 1-MA. Error bars are 95% confidence intervals. There appears to be an annual cycle, with peak oocyte sizes in the late autumn to mid-late spring. All mature oocytes were >155 μm on average.

Developmental table and staging

Pycnopodia helianthoides proceeds through embryogenesis, bipinnaria, and brachiolaria stages according to the developmental schedule shown in Table 2, a faster rate than previously reported (Greer, 1962). Selected embryo and larval stages are shown in Figure 3. Brachiolariae have notably long arms, especially the posterolateral arms, which can be significantly longer than the larval body length. As is true for many sea stars (reviewed in Allen *et al.*, 2018), cloning in *P. helianthoides* larvae was commonplace: we observed clones in all larval cultures.

Juvenile skeleton first appeared in the rudiment of larvae from WA parents at ~27 dpf (Fig. 4A). Radial canals appeared successively, starting at ~39 dpf (Fig. 4B). At ~43 dpf, the buds that will form the brachiolar arms are visible in the most advanced larvae (Fig. 4F); we consider this the beginning of the brachiolar stage. At ~51 dpf, larvae exhibit skeletal rings around their posterior periphery, resembling a helmet (Figs. 3I, 4G). We refer to this as the helmet stage and use the prominence of the helmet as a way of tracking the approach of larvae to competence (Fig. 4I). At around this same time, *bona fide* brachiolar arms are present in most larvae (Fig. 4J), as are long posterolateral arms, often longer than the entire body length (see, *e.g.*, Figs. 3I, 4G).

To further characterize late larval development in *P. helianthoides*, we developed a staging scheme based upon formation of the aforementioned and other skeletal structures in the rudiments of advanced larvae, which, along with simultaneous events in the maturation of the brachiolar apparatus, can be used to monitor the approach to metamorphic competence in a batch of larvae (Table 2; Fig. 4).

We reared larvae at 11 °C and 14 °C (WA parents); those reared at 14 °C developed more rapidly (data not shown). Therefore, it should be noted that the timeline in Table 2 is likely very temperature dependent, and time to competence and interim stages would likely be significantly reduced at higher temperatures.

Settlement observations and experiments, including turbulence exposures

Competent *P. helianthoides* larvae will settle spontaneously on the sides of the culture vessels and will do so more readily if a biofilm is allowed to form on the jars. We first observed such spontaneous settlement starting about 7 wk post-fertilization (pf) in larvae reared at 10–11 °C. Peak spontaneous settlement appeared to have occurred earlier in larvae derived from AK parents when compared to WA-derived larvae (week 8 pf *vs.* week 11 pf; Fig. 5), possibly pointing to different temperature optima in populations across the species range. However, the later spontaneous settlement seen in larvae derived from WA parents in Figure 5 may have been due to our more intense jar exchange and cleaning regime—resulting in a less well-developed biofilm—when culturing these latter larvae.

We identified four phases in the settlement process (Fig. 6):

1. In the exploration phase (not shown), the larva will swim freely and occasionally remain in contact with the walls of the jar or a settlement surface, such as a frond of coralline alga, and then resume swimming.

2. In the attachment phase (Fig. 6A), the larva will adhere to a surface by using its brachiolar apparatus. Larvae in the

Table 2

Developmental stages in Washington Pycnopodia helianthoides*, 10–11 °C, including proposed rudiment staging scheme for late larval development (RS-1 to RS-5)*

Stage	Time	Figure reference
Fertilization	0 hpf	
First cleavage	5 hpf	Fig. 3D
Second cleavage	6 hpf	
Hatching	44 hpf	
Gastrulation	50 hpf	Fig. 3E
Early bipinnaria (can feed)	6 dpf	Fig. 3F
Mid-bipinnaria, anterior fusion of enterocoels	17 dpf	Fig. 3G
Late bipinnaria, posterior fusion of enterocoels; RS-1: first appearance of juvenile skeleton in rudiment; wishbone spicules (incipient body skeletal plates) present in most advanced larvae	27 dpf	Figs. 3H, 4A
RS-2: first appearance of radial canals (pentamery beginning to develop through successive formation of the five radial canals *via* hydrocoel bumps)	39 dpf	Fig. 4B
Early brachiolaria larva (brachiolar arm buds visible, adhesive disk forming); RS-3: skeletal elements forming at lateral edges of radial canals; body skeletal plates now at snowflake stage	43 dpf	Fig. 4D, 4E, 4F
Brachiolar adhesive disk developing, lateral papillae forming; RS-4: helmet forming at posterior periphery *via* peripheral spicules; stellar arrangement of spicules around snowflake body skeletal plates	51 dpf	Figs. 3I, 4G, 4H
Competent larva; adhesive papillae on brachiolar arms well developed; RS-5: bumped appearance of helmet from expanding peripheral skeletal spicules	55 dpf	Fig. 4I, 4J

Alaska *P. helianthoides* larvae proceeded through these stages slightly more quickly at the same temperature (data not shown). dpf, days post-fertilization; hpf, hours post-fertilization; RS, rudiment stage.

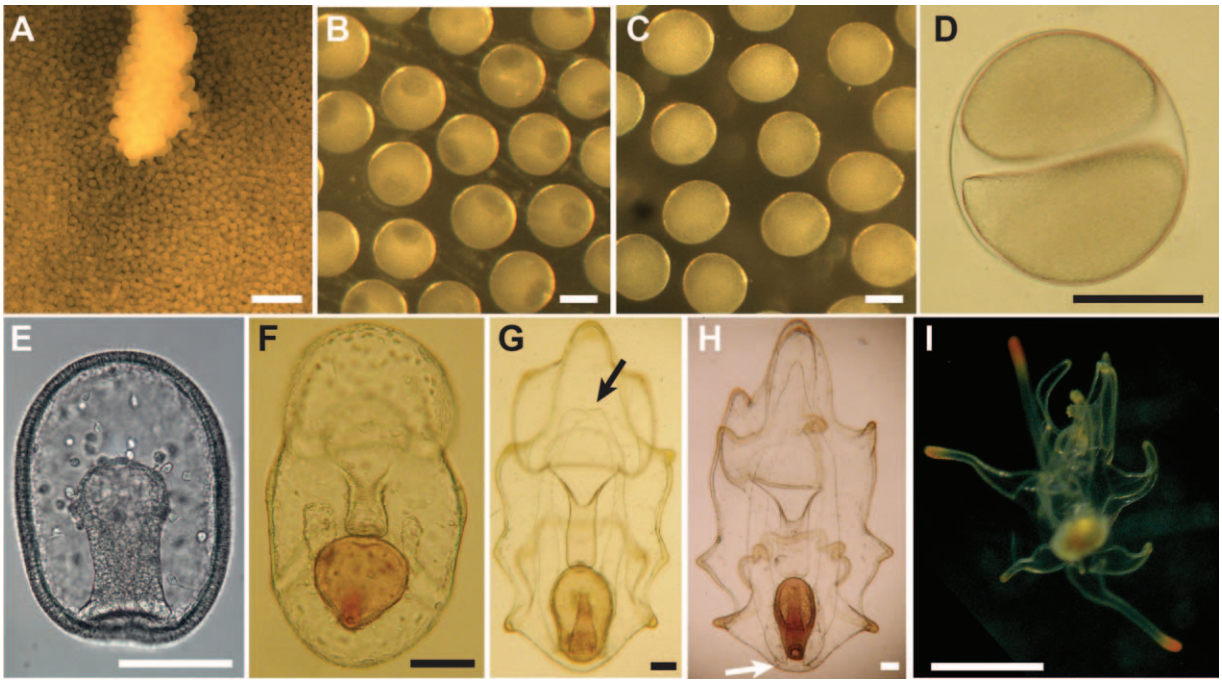

Figure 3. Oocyte maturation, embryogenesis, and larval development in *Pycnopodia helianthoides*. (A) Ovary releasing (spawning) mature oocytes in response to 1-methyladenine (1-MA). (B) Just-released oocytes with intact germinal vesicles (clear areas within oocytes). (C) At 1.5 h later, after germinal vesicle breakdown (GVBD), these eggs are now fertilizable. (D) Two-cell stage, 5 hours post-fertilization. (E) Mid-gastrula, 3 days post-fertilization (dpf). (F) Early-feeding bipinnaria larva, 7 dpf; gut red from *Rhodomonas*. (G) Mid-bipinnaria, 17 dpf; enterocoels are just fusing anteriorly (black arrow). (H) Late bipinnaria, 26 dpf; enterocoels are almost fused posteriorly (white arrow). (I) Swimming brachiolaria larva, 41 dpf. Scale bars in (A) and (I) = 1 mm; all other panels = 0.1 mm.

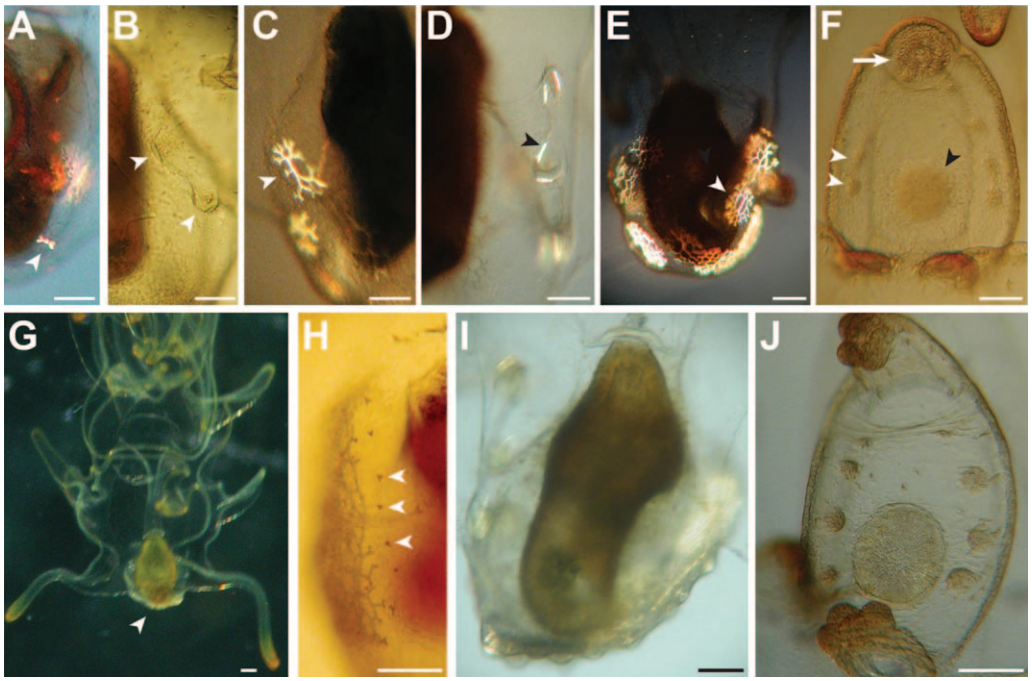

Figure 4. Characters used to define proposed rudiment stages (RS) and correlated late-stage larval characters of *Pycnopodia helianthoides*. (A) Posterior right side of the larva, dorsal view. Incipient juvenile body skeletal plates initially form multi-branched spicules in the form of a wishbone (white arrowhead), characteristic of RS-1. (B) Posterior left side of the larva, ventral view. Radial canals form as out-pocketings of the hydrocoel in RS-2, the first signs of fivefold symmetry. White arrowheads denote two visible radial canal anlagen. (C) Posterior right side of the larva, ventral view. Here the wishbone structure seen in (A) is further bifurcating as it grows (white arrowhead). (D) Posterior left side of the larva, ventral view. Skeletal spicules (black arrowhead) are visible along the lateral edges of the extending radial canals, characteristic of RS-3. (E) Posterior end of the larva, dorsal view. The wishbone structure seen in (A) and (C) has further elaborated into what we term the snowflake form (white arrowhead), also characteristic of RS-3. (F) Anterior end of the larva, ventral view. Coincident with RS-3, the brachiolar arms are forming as buds but have not yet developed adhesive papillae (white arrow). The adhesive disk of the incipient attachment complex (see Haesaerts *et al.*, 2005) is here coalescing (black arrowhead). Five anlagen of the lateral papillae of the attachment complex are visible in this larva as well (two indicated with white arrowheads). (G) Ventral view, indicating that the helmet structure (white arrowhead), characteristic of RS-4 and comprised of spicules at the posterior periphery, is visible in this binocular microscope image. (H) Posterior right side of the larva, ventral view. White arrowheads indicate three elements of the stellar array of spicules that forms around the further elaborated (snowflake) body skeletal plates in RS-4. (I) Posterior end of the larva, ventral view. In RS-5, the helmet takes on a clear, bumpy appearance, resulting from the growing spicules in the helmet. (J) Anterior end of the larva, ventral view. Coincident with RS-5, the brachiolar arms are now fully formed with adhesive papillae, the adhesive disk is mature and birefringent, and there are now eight lateral papillae visible (*cf.*, F). (A), (C–E), (I), and (J) employed cross-polarized light to highlight spicules. Scale bars = 100 μm.

attachment stage can remain in this stage for extended periods (24 h or more), can detach and return to the exploration phase, or can proceed to the settler phase.

3. In the settler phase (Fig. 6B), the larva has irreversibly committed to settling. The larval body shrinks along its anterior-posterior axis, and the length of the larval arms (this is particularly noticeable in the posterolateral arms) shrinks dramatically as well.

4. In the settled stage (Fig. 6C, D), which occurs ~24–48 h after the larva commits to the settler phase, we consider it to be a *bona fide* juvenile. The larval body has withdrawn completely into the aboral surface of the juvenile. Soon, the juvenile begins to adhere to the surface with tube feet instead of the brachiolar apparatus and can move freely on the substratum. Settled juveniles will continue metamorphosis for several days until their mouths are open.

In addition to the spontaneous settlement described above, larvae will settle at low levels in response to a variety of natural biofilms (Fig. 7), including biofilms grown in the presence of either of two *P. helianthoides* prey species, purple urchins (*Strongylocentrotus purpuratus*; Fig. 7C) or mussels (*Mytilus* spp.; Fig. 7B), or in the absence of any macroinvertebrates (general biofilm; Fig. 7A). By contrast, biofilm grown in the presence of *P. helianthoides* adults results in q11

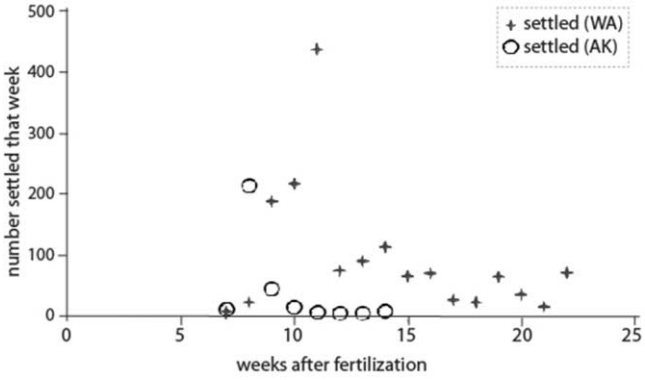

Figure 5. Spontaneous settlement in *Pycnopodia helianthoides* larvae derived from Alaska (AK) or Washington (WA) adults. Open circles indicate AK larvae (summer–autumn 2019); plus symbols indicate WA larvae (autumn–winter 2019–2020). Note that we cultured many fewer total AK larvae than we did WA larvae.

both a faster and more robust settlement response when compared to any of these other biofilms (Fig. 7A–C; see figure legend for statistics). Exposure of larvae to live fronds of the articulated coralline alga, *Calliarthron tuberculosum*, results in comparably enhanced settlement ($Z = 8.751$; $P < 0.001$; Fig. 7C). The potency of *P. helianthoides*-associated biofilm degrades over time as the biofilm ages in MFSW in the absence of the adult stars ($Z = 4.654$; $P < 0.001$; Fig. 7D).

We also examined settlement behavior following turbulence exposure, a condition that may signal to larvae that they are approaching the shoreline, where turbulence levels increase (for review see Hodin *et al.*, 2018). We assessed three behaviors in response to turbulence: a temporary knockdown of larvae to the substratum (see Hodin *et al.*, 2020), attachment of larvae onto the substratum, and the rate of subsequent irreversible settlement. Following turbulence exposure, the quantifiable (5 W kg^{-1} in a Taylor-Couette device) and qualitative (shaking) treatments resulted in a threefold increase in larval knockdown when compared to controls ($Z = 6.111$; $P < 0.001$; Fig. 8A); we did not detect a difference between the two turbulence treatments ($Z = 1.606$; $P = 0.44$; Fig. 8A). Likewise, after 1 h in a strong settlement inducer (*P. helianthoides* biofilm), the larvae in both turbulence treatments exhibited an approximate 2-fold increase in irreversible settlement when compared to controls ($Z = 3.433$; $P < 0.005$; Fig. 8B, open bars). Again, we detected no difference between the 2 turbulence treatments in irreversible settlement at 1 h ($Z = 0.185$; $P > 0.5$; Fig. 8B, open bars). We obtained comparable results at 1 h for larval attachment (data not shown), a reversible stage of the settlement process. By 24 h after exposure, we no longer detected a difference in settlement between any of the treatments ($Z = 1.716$; $P > 0.5$; Fig. 8B, filled bars). Together, these results suggest that turbulence exposure heightens larval responses to settlement inducers but does not change the proportion of larvae that will ultimately settle. in response to these inducers.

Juvenile survival, feeding, and growth

In early juvenile stages, *P. helianthoides* has a rounded, dome-like shape (Fig. 9A). As it matures, it becomes dorsal ventrally compressed and pentagonal in form, and distinct radial arms begin to develop (Fig. 9B). Additional arms are added periodically by one of three methods (from most to least common): (1) a new arm emerging from an armpit (Fig. 9D, E); (2) sagittal bifurcation of an existing arm (Fig. 9D); or (3) lateral budding of a new arm (Fig. 9C; observed only once). Some juveniles initially developed fewer than five arms (Fig. 9E, H). We have observed several such juveniles eventually form their fifth and add subsequent arms as they continue to grow (*e.g.*, Fig. 9E, H).

Juveniles lose their larval pigmentation and their coloration may fade or change in response to their diet; once larval pigment fades, the juvenile gut appears clear. As juveniles successfully feed and grow, color can be seen in the stomach

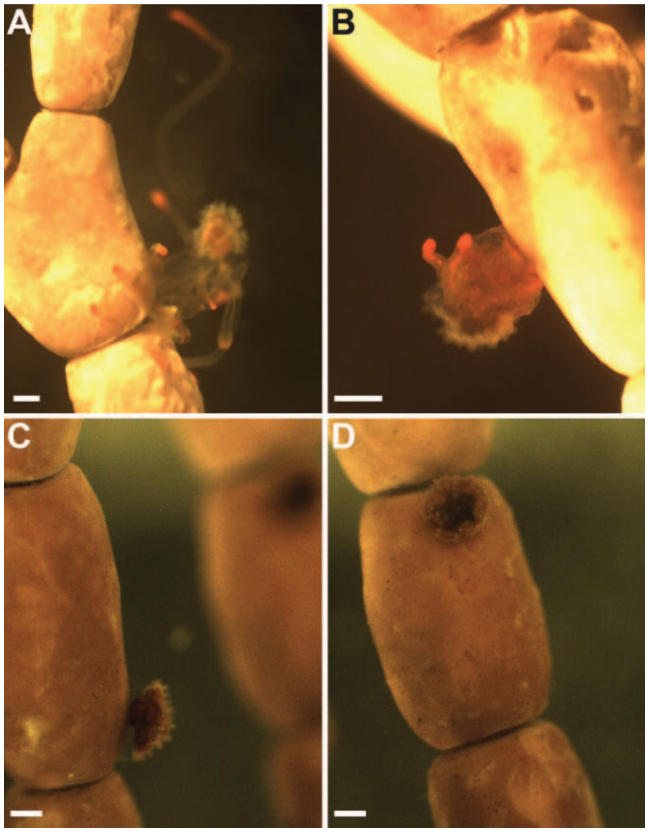

Figure 6. Phases of settlement in *Pycnopodia helianthoides*. The first phase is exploration (not shown). (A) Attachment phase, lateral view. Larva adheres to a frond of coralline algae (*Calliarthron tuberculosum*) with brachiolar arms and waves its posterolateral arms. (B) Settler phase, lateral view. Irreversible settlement commences with adhesive disk attachment and retraction (collapse) of larval body along the anterior-posterior axis. (C) Settled phase, lateral view. Larval body has been completely withdrawn. Juvenile will soon move with tube feet. (D) Recently settled juvenile, aboral view, exhibiting first indications of arm development (note pentamery in the incipient juvenile gut). Scale bars = 250 μm.

see following page for readable version of this figure.

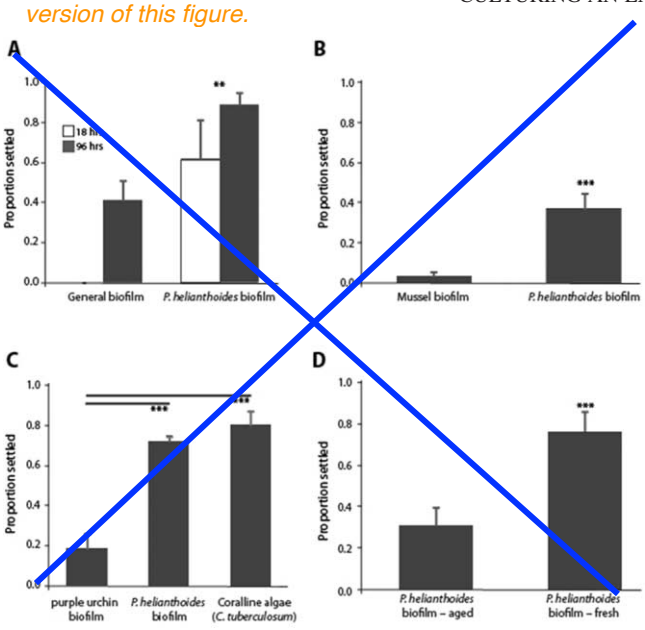

Figure 7. Settlement of *Pycnopodia helianthoides* on various substrata. (A) Alaska (AK) larvae. (B–D) Washington (WA) larvae. (A) Experiment 1 (68 days post-fertilization [dpf]; 18- and 96-h exposure): larvae settled both more quickly (open bar; $F_{1,8} = 9.263$; $P = 0.016$) and in higher numbers (filled bars; $F_{1,8} = 23.459$; $P = 0.0013$) when exposed to biofilm grown in the presence of conspecific adults, as compared to general biofilm (*i.e.*, no macroinvertebrates present). (B) Experiment 2 (86 dpf; 24-h exposure; 4 replicates [reps] per treatment; 20 larvae per rep): this response to conspecific biofilm was not due to the confounding effect of the presence of their prey (*Mytilus edulis* mussels; $Z = 5.357$; $P < 0.001$). (C) Experiment 3 (134 dpf; 50-h exposure; 4 reps per treatment, $n = 30$ larvae per rep): larvae also responded more readily to fronds of an articulated coralline alga (*Calliarthron tuberculosum*) or to conspecific biofilm ($Z = 5.250$; $P < 0.001$) when compared to biofilm grown in the presence of another known adult prey species, the purple urchin, *Strongylocentrotus purpuratus*. (D) Experiment 4 (73 dpf; 96-h exposure; 4 reps per treatment; 20 larvae per rep): the conspecific biofilm is much more active when freshly collected (tested 9 d after exposure to adults), compared to similar biofilm aged for 25 d after exposure to adults. "Settled" in all panels includes both settlers and settled phase larvae. Error bars = SEM. $^{**}P < 0.01$; $^{***}P < 0.001$.

(presumably from digesting food); and gut development can then be monitored as juveniles grow: the incipient pyloric coeca can be seen growing down the arms of live juveniles and then bifurcating (*e.g.*, Fig. 9B, I, N).

When *P. helianthoides* juveniles were maintained on biofilm with or without coralline algae, they did appear to be consuming something, as indicated by the slight darkening of their guts after a few weeks. Nevertheless, they did not exhibit significant growth under these conditions, indicating that this minimal consumption may have simply been sufficient for metabolic maintenance rather than growth *per se*.

For juveniles derived from AK parents, starting at 35 d post-settlement we assessed growth and survival over 50 d, during which time juveniles were fed 1 of 3 potential food sources: juvenile sand dollars, Otohime (a commercial fish diet; Pentair Aquatic Eco-Systems), or crushed cockles. Controls did not receive any supplemental food aside from the biofilm present in the treatment vessels at the onset of the experiment (see *Materials and Methods*). Each treatment vessel had 2 *P. helianthoides* juveniles at the beginning of the experiment, and by day 50 there were always either 1 or 2 juveniles remaining. In one case (a control vessel) we observed a cannibalism event, thus accounting for the disappearance of one juvenile. In the other cases of juvenile disappearance, we presume that the remaining juvenile consumed its partner, but we are unsure whether these other cases were due to cannibalism or scavenging on an already dead juvenile. After 50 d, we detected no differences between treatments either in mortality ($Z = 0.800$; $P > 0.4$) or in final juvenile size ($F_{3,8} = 1.436$; $P = 0.3$). Nevertheless, when we grouped vessels regardless of treatment by numbers of juveniles remaining (one or two), we detected a

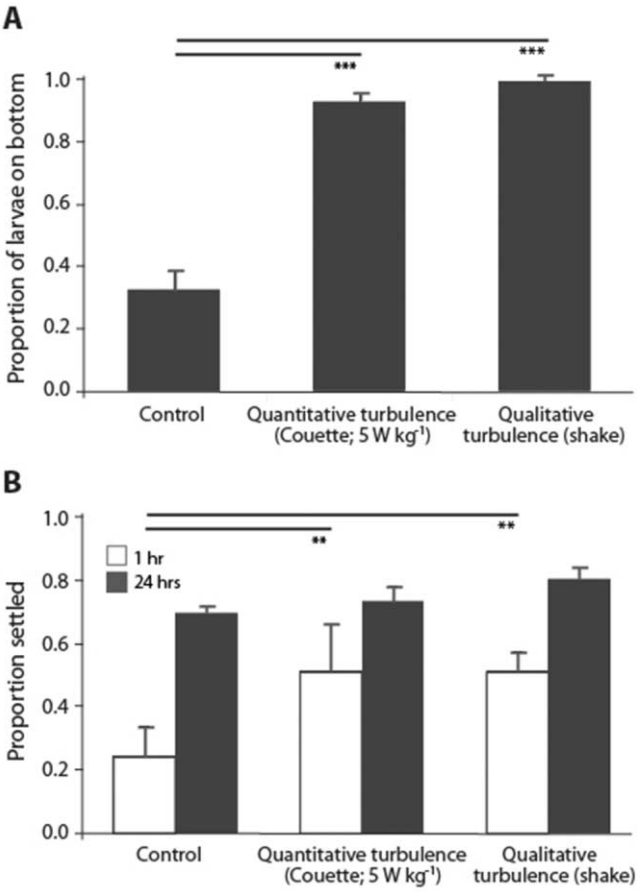

Figure 8. Turbulence promotes rapid settlement behaviors in *Pycnopodia helianthoides*. (A) Immediately following 3 min of either 5 W kg^{-1} exposure in a Taylor-Couette device (quantitative turbulence) or shaking of larvae in a flask (qualitative turbulence), about 3-fold more larvae were knocked down to the substratum when compared to controls (4 replicates [reps] per treatment; $n =$ 25–30 larvae per rep). (B) Then, 1 h later, about 2-fold more turbulence-exposed larvae were in the process of irreversibly settling in response to conspecific biofilm as compared to controls (open bars). By 24 h, similar proportions of larvae were settling in all treatments (filled bars). Error bars = SEM. $^{**}P < 0.01$; $^{***}P < 0.001$.

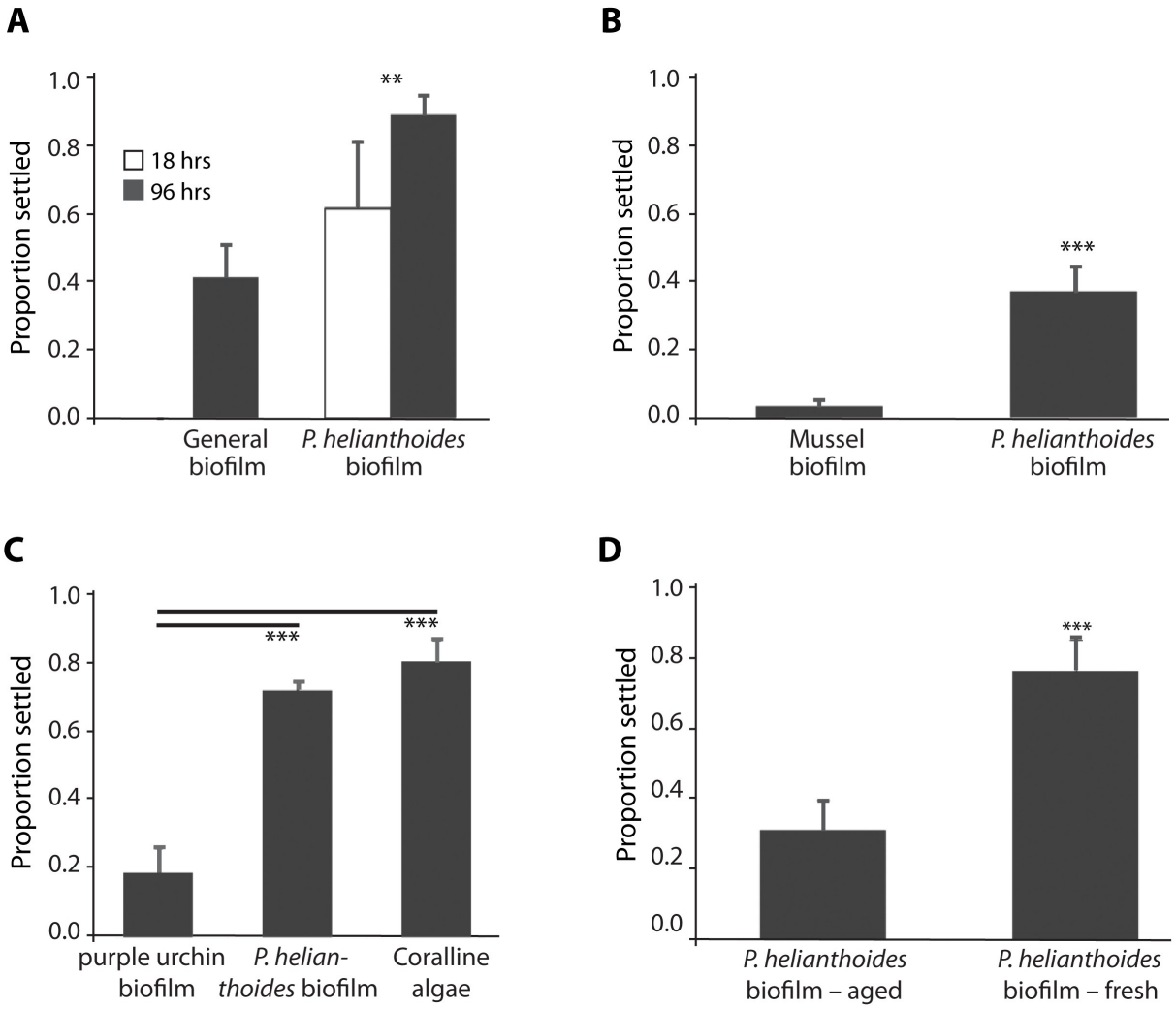

Figure 7. Settlement of *Pycnopodia helianthoides* on various substrata. (A) Alaska (AK) larvae. (B–D) Washington (WA) larvae. (A) Experiment 1 (68 days post-fertilization [dpf]; 18- and 96-h exposure): larvae settled both more quickly (open bar; $F_{1, 8} = 9.263$; $P = 0.016$) and in higher numbers (filled bars; $F_{1, 8} = 23.459$; $P = 0.0013$) when exposed to biofilm grown in the presence of conspecific adults, as compared to general biofilm (i.e., no macroinvertebrates present). (B) Experiment 2 (86 dpf; 24-h exposure; 4 replicates [reps] per treatment; $n = 20$ larvae per rep): this response to conspecific biofilm was not due to the confounding effect of the presence of their prey (*Mytilus edulis* mussels; $Z = 5.357$; $P < 0.001$). (C) Experiment 3 (134 dpf; 50-h exposure; 4 reps per treatment, $n = 30$ larvae per rep): larvae also responded more readily to fronds of an articulated coralline alga (*Calliarthron tuberculosum*) or to conspecific biofilm ($Z = 5.250$; $P < 0.001$) when compared to biofilm grown in the presence of another known adult prey species, the purple urchin, *Strongylocentrotus purpuratus*. (D) Experiment 4 (73 dpf; 96-h exposure; 4 reps per treatment; $n = 20$ larvae per rep): the conspecific biofilm is much more active when freshly collected (tested 9 d after exposure to adults), compared to similar biofilm aged for 25 d after exposure to adults. "Settled" in all panels includes both settlers and settled phase larvae. Error bars = SEM. $^{**}P < 0.01$; $^{***}P < 0.001$.

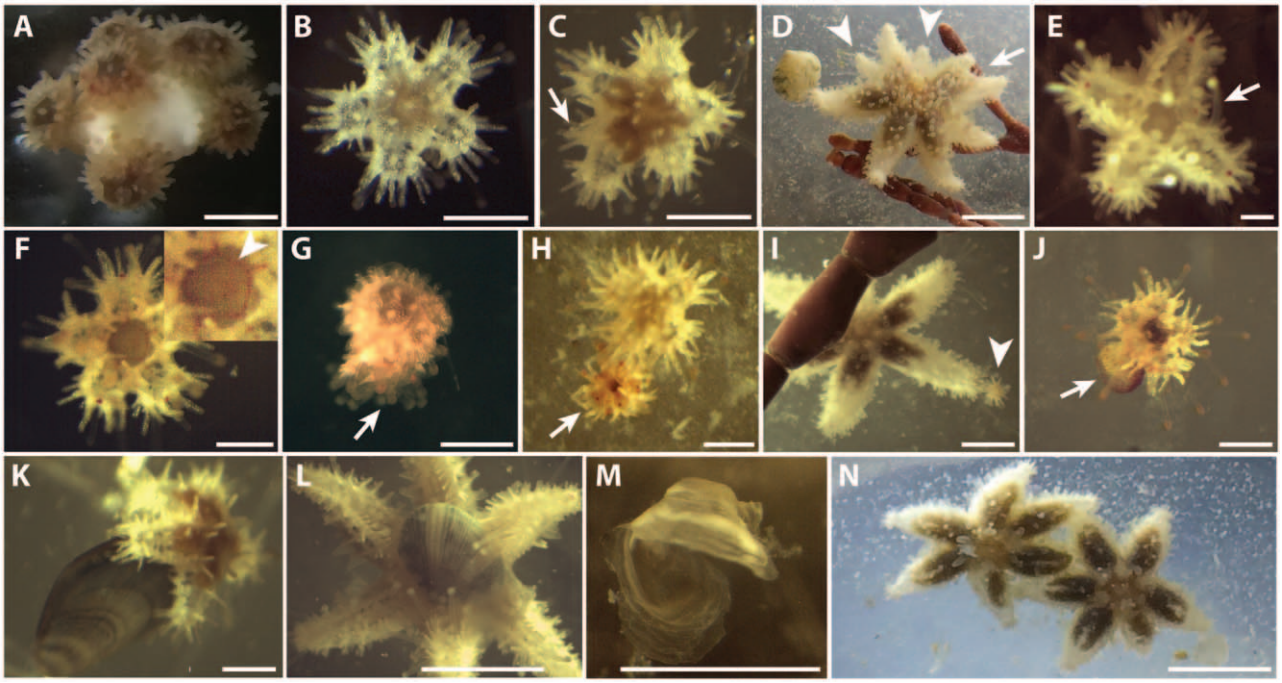

Figure 9. Early juvenile ontogeny of *Pycnopodia helianthoides*. Unless indicated, all photos are of Washington (WA)-derived juveniles and are aboral views. Brown areas are gut, and pyloric caeca are seen through the body wall. Time in months (mo) is age post-settlement. (A) Cluster of newly settled juveniles on a dead piece of coralline algae. (B) Alaska (AK)-derived juvenile, 3 mo, with the typical 5 initial arms. (C–E) Three methods of new arm formation. (C) Lateral bud (arrow), 2 mo. This is the only star we observed forming a new arm in this manner. (D) This 7-mo juvenile exhibits the other 2 methods of new arm formation: sprouting of new arms from armpits (most common; arrowheads), and sagittal bifurcation of an existing arm (arrow). (E) Aberrant (though not very rare) 4-arm juvenile, oral view, forming its fifth arm from armpit (arrow) at 4 mo. Note the red eyespots at the tips of each arm, including the incipient fifth one. (F) Pigment cells outlining the nerve ring (arrowhead in magnified inset), oral view, 3 mo. (G–M) Juveniles feeding. (G) Cannibalism. Arrow indicates tube feet of living juvenile being cannibalized by the 2-mo AK-derived juvenile on top. (H) This 9-mo, 4-arm juvenile (note that broad fourth arm at upper left is preparing to bifurcate) is scavenging a dead conspecific. (I) This 5-mo juvenile under a frond of coralline algae is bringing in a dead purple urchin juvenile (arrowhead) with its tube feet. (J) Slowly growing 4-mo juvenile preparing to consume a live, precocious purple urchin juvenile (arrow) that settled without spines. (K) Unsuccessful attempt by 4-mo juvenile to consume a juvenile mussel (epizoite on coralline alga). (L) Oral view, 9 mo, successful predation underway on a live Manila clam juvenile. (M) Results of successful predation on a live Pacific oyster juvenile. (N) Juvenile cage mates, 8 mo, exhibiting typical gregarious behavior, similar to that seen in adults. Note the extensive migration of pyloric caeca down the arms of these stars relative to juveniles in other panels. All scale bars = 0.5 mm, except 5 mm in (D), (I), (K–N).

difference in juvenile size ($F_{1,10} = 8.498$; $P < 0.02$): juveniles in vessels with 1 survivor had a mean diameter ± SEM of 741 ± 66 μm as compared to a mean diameter of 594 ± 28 μm when both juveniles survived. In other words, cannibalism or conspecific scavenging resulted in clearer evidence for juvenile growth than did feeding on any of the provided food sources. Qualitatively, the juveniles fed cockles appeared generally healthier than in any of the other treatments, and this was the only treatment exhibiting zero mortality (see *Materials and Methods* for criteria employed to assess juvenile health).

Preliminary observations on juvenile feeding. Juveniles under flow conditions appeared more robust and more active. The juveniles consumed living and dead organisms, including echinoid juveniles (the Pacific sand dollar *Dendraster excentricus* and the purple urchin, *S. purpuratus*), bivalve juveniles (mussels [*Mytilus* spp.], Manila clams, and Pacific oysters), and conspecific juveniles (*P. helianthoides*). Our observations indicate that *P. helianthoides* juveniles actively prey or scavenge on the echinoderm juveniles earlier in juvenile ontogeny than when they begin to prey upon the bivalves. They also feed on bivalve tissues before they are capable of opening the shells (we observed several juveniles attempt unsuccessfully to open a mussel and only after many weeks of trying finally succeed).

Once juveniles reach 1–2 mm in diameter, they will readily feed on tissue of Manila clams and Pacific oysters; at ~1 cm in diameter, they will begin to successfully open and feed on these bivalve species (shell length = 1–2 mm) and will consume

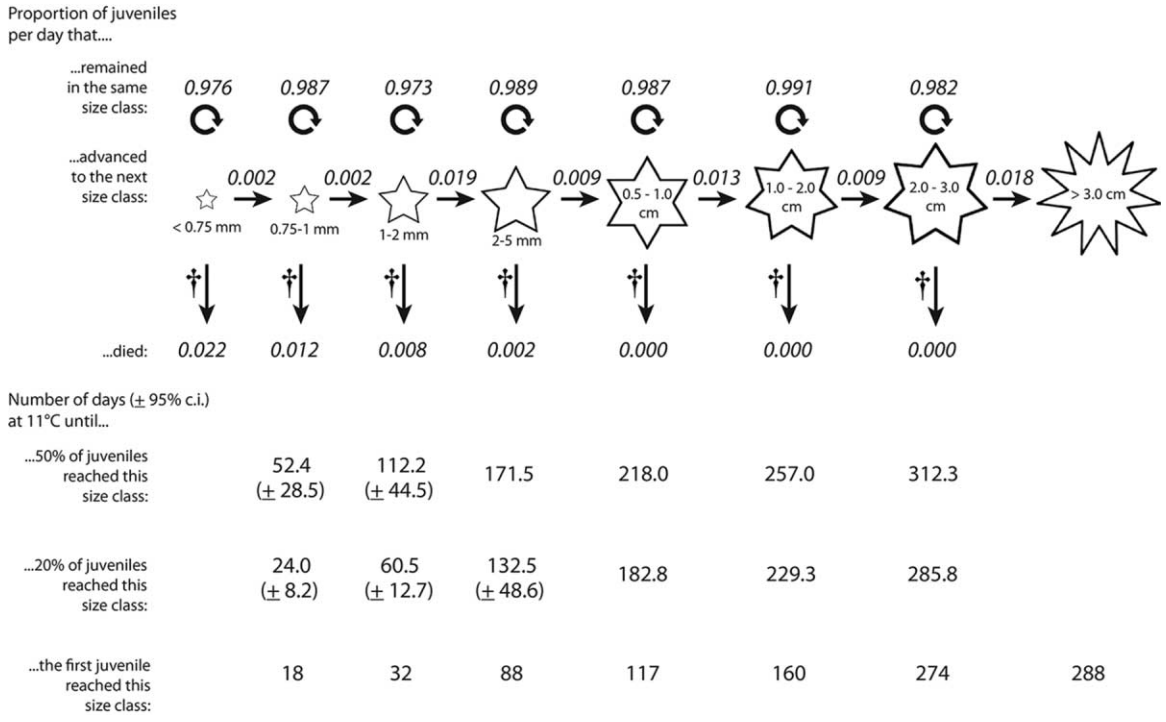

Figure 10. Model of juvenile growth and survival in *Pycnopodia helianthoides*. We here summarize our growth and survival data in the form of a modified Lefkovitch model (Lefkovitch, 1965). Put simply, we periodically counted and measured every juvenile in our rearing chambers and from these data calculated the likelihood of a given larva surviving and growing into a subsequent size class between sampling dates. We made the simplifying assumption that individual juveniles within a chamber maintained their relative rank order of sizes between measurements. We also assumed, unless there was specific evidence to the contrary, that if juveniles disappeared between observation dates, it was the smaller individuals that were most likely to have perished. The data in the upper half of the figure support the conclusion that mortality is highest at smaller sizes (with the caveat that the aforementioned survival-by-size assumption slightly biases this conclusion) and that growth accelerated at larger sizes. Data in the bottom half of the figure resulted from the same analysis. The 95% confidence ranges are not available for the larger size classes because midway through our observation period, we separated juveniles by size class to limit cannibalism. The result was that we no longer had replicate chambers of the different size classes at larger juvenile sizes.

other live invertebrates as well (*e.g.*, juvenile limpets) if given the opportunity. The relationship between the diameter of *P. helianthoides* juveniles and the volume of bivalves consumed per day can be found in Figure ~~S4~~ (data supplement, available online). *Pycnopodia helianthoides* juveniles at >1 mm will also readily feed on sand dollar and purple urchin juveniles.

Initial survival was poor, and growth was slow (Fig. 10; Figs. ~~S2, S3~~, data supplement, available online). We attribute these findings to the fact that during these early juvenile stages, we were investigating and adjusting vessel design, flow conditions, water filtration, and possible food sources, none of which have been optimized previously for any sea star of which we are aware.

Figure 10 summarizes our growth and survival data in the form of a model (akin to a Lefkovitch matrix; Lefkovitch, 1965). The upper half of the figure indicates the daily likelihood of a given juvenile dying, remaining in the same size class, or advancing to the next size class. Although we have seen the rare individual juvenile shrinking slightly between measurements, we never observed an individual regressing to a prior size class (data not shown). These data are consistent with the survival (Fig. ~~S2~~, data supplement, available online) and growth (Fig. ~~S3~~, data supplement, available online) figures, showing high mortality and slow growth early, with increases in both juvenile survival and growth rates at larger sizes.

The lower half of Figure 10 gives an approximate ontogenetic growth schedule, summarizing the number of days post-settlement that it took for 50% of the surviving juveniles, 20% of the surviving juveniles, or the first juvenile to reach a given size class. We present this range of growth schedules in light of our uncertainty regarding the suitability of the initial growth conditions used.

Discussion

We report on successful culturing of the endangered sunflower star, *Pycnopodia helianthoides* Brandt, from egg to 1 yr

post-settlement juvenile. Our goal is to establish egg-to-egg full life cycle culturing in captivity, with three long-term objectives in mind. First, captive rearing can promote further studies in the ontogeny, physiology, and ecology of this key benthic predator, while obviating the necessity of collecting this endangered species from the wild. Second, by developing methods to culture *P. helianthoides* juveniles for the first time, we now have access to these cryptic life stages for investigations into their growth, feeding ecology, and behavior. And, third, because sunflower stars are thought to be extirpated, or nearly so, from almost half of their historical range in the NE Pacific, our captive rearing program represents the first step in a collective exploration of the eventual feasibility of their reintroduction into the wild.

We obtained mature oocytes from amputated *P. helianthoides* arms; the standard method to obtain eggs by injection of the sea star spawning hormone 1-MA had limited success. The stars recovered from amputations, as evidenced by regenerating arms, completion of additional reproductive cycles the year after amputation, and no observed mortality or other health issues following amputation. Because we can distinguish individual adult stars based on their color patterns (see Fig. 1; Fig. S1, data supplement, available online), we have been able to more efficiently undertake amputations, because we now know the sex of 24 of our 28 captive stars.

Prior studies stated that mature eggs of *P. helianthoides* were ~120 μm in diameter (Greer, 1962; Strathmann, 1987), but we could not find primary data to support this assertion. Our data for *P. helianthoides* from both AK and WA populations show that the egg size in *P. helianthoides* is 155–170 μm in diameter, which is consistent with the one measurement of a fertilized *P. helianthoides* egg of which we are aware (G. von Dassow, University of Oregon, pers. comm.) prior to the recent SSW event. Therefore, it does not seem that egg sizes have changed in *P. helianthoides* populations in response to the recent SSW event. We have observed the rare egg within a batch that was smaller than 155 μm and successfully matured and fertilized. Nevertheless, when the maximum oocyte size for a given female was less than 150 μm, the oocytes failed to mature and, thus, remained unfertilizable.

We also noted differences from the literature in the timing of reproductive maturity in sunflower stars in the San Juan Archipelago. Strathmann (1987 and references therein) gave the timing of mature oocytes as March–July, with peak spawning in the field in May–June. By contrast, we have seen mature oocytes as early as November and little evidence for mature oocytes after April–May. We observed four spontaneous spawning events in captivity, all between March and May, which is a bit earlier than the peak spawning timing noted in Strathmann (1987). It is possible that the earlier reproductive maturity we observed is a recent shift, possibly associated with SSW. Furthermore, we have noted that recently collected stars, even when reproductively mature, tended to have small gonads (a few centimeters in length), relative to what is seen in other sympatric asteroids (JH, pers. obs.). This may also be a consequence of SSW (*e.g.*, a trade-off between survival and reproduction in the face of the disorder). In sum, we advocate amputations for reproductive studies in WA in the winter and early spring. Our one data point on stars in AK suggests a later reproductive season in those colder northern waters.

As stated above, our data indicate that captive adult stars completed a reproductive cycle (and, thus, became reproductive again) while in captivity. In response to 1-MA treatment, mature oocytes in isolated gonads underwent GVBD, eggs were successfully fertilized, and we reared larvae through metamorphosis and settlement following established protocols (Adams *et al.*, 2019; Hodin *et al.*, 2019). Progression through embryonic and larval stages was as described by Greer (1962), though larval development proceeded more rapidly under our growth conditions. We first observed settlement beginning in cultures 7 wk pf at 10–11 °C, 2 wk earlier than reported by Greer (1962) at similar temperatures. Competent larvae will settle spontaneously and in response to a variety of natural biofilms, but settlement proportions and rates are greatly enhanced in response to a biofilm collected in the presence of adult sunflower stars or if larvae are exposed to fronds of the articulated coralline alga, *Calliarthron tuberculosum*. The combination of these two cues seems to enhance settlement even further. We also found that turbulence exposure induces a more rapid and synchronous settlement response to the aforementioned cues, which could be a useful technique in any large-scale rearing effort.

Our greatest challenges have occurred in developing suitable protocols for juvenile rearing, a process that has been successfully reported in the past for only a handful of asteroid species with planktotrophic development (*e.g.*, the New Zealand sea star *Stichaster australis*; Barker, 1979). Our juvenile cultures experienced high initial mortality rates due to a variety of likely causes (see *Materials and Methods*, *Results*, and data supplement, available online, for details). With optimization of methods, we were able to stabilize this mortality, and the juveniles began to grow rapidly. We had the greatest success when we cultured juveniles in micron-filtered natural seawater in flow-through cages and fed them juvenile bivalves.

We note that the juvenile growth pattern that we observed—slow initial growth for the first months after settlement, followed by more rapid growth after (see Figs. ~~S2, S3~~, data supplement, available online)—is reminiscent of observations on juvenile growth in ~~two~~ other sea stars: the temperate NE Atlantic species *Asterias rubens* (Nauen 1978), and the tropical S Pacific crown-of-thorns sea star, *Acanthaster* spp. (Deaker *et al.*, 2020). In both cases, the juveniles seem to have the ability to persist for long periods under suboptimal growth conditions as a waiting period until better conditions arise, such as their encountering a prime prey species. We do not yet know, however, whether this waiting period for sunflower star juveniles is facultative or obligate, since we have not yet had the

S3, S4

three

(insert above at ^ mark): "...and Marthasterias glacialis (Byrne et al. 2021), ..."

opportunity to provide them optimal food and growth conditions from immediately after settlement. We plan to assess these scenarios in the coming year.

q16 Importantly, we observed for the first time young *P. helianthoides* juveniles (a few months post-settlement; <1-cm diameter) actively consuming living echinoid juveniles (sea urchins and sand dollars; <2-mm diameter). Juvenile and adult red (*Mesocentrotus franciscanus*), purple (*Strongylocentrotus purpuratus*), and green (*Strongylocentrotus droebachiensis*) sea urchins are all known prey of adult sunflower stars (Mauzey *et al.*, 1968; Dayton, 1975; Moitoza and Phillips, 1979; Duggins, 1983; Freeman, 2005; Nishizaki and Ackerman, 2007). Our observations raise the possibility that *P. helianthoides* could exert top-down predatory control in the wild on these urchin species, starting at early juvenile stages in both predator and prey. This intriguing hypothesis remains to be tested.

We conclude by advocating that species reintroductions should truly be considered the solution of last resort when it comes to ensuring the persistence of species in their natural habitats. And while the long-term possibility of sunflower star reintroductions is a credible consideration, our primary objective in this captive-rearing effort is to learn more about the basic biology and ecology of this endangered predator. We see this approach as not only adding to our general knowledge of benthic biology and ecology but also informing other conservation interventions designed to protect this species in the wild and encourage its return. We further hope that our studies highlight the importance of basic research into poorly understood marine taxa so that critical information about such species' biological and ecological functions are known before the next SSW-like calamity strikes.

Acknowledgments

We are extremely grateful for the diverse assistance we have received from so many people in various aspects of the project. We first thank Sherry Tamone and lab for collecting Alaskan stars, isolating gonads, and shipping them to us for our first successful sunflower star fertilizations. We further thank John Dorsett, Willem Weertman, Joey Ullman, Hank Carlson, Taylor Frierson, Jon Allen and team, Mo Turner, ZooBots 2019, Jim Murray, Sadie Youngstrom, Olivia Graham, Frank Hurd, Richard Emlet, Katie Dobkowski, Tim Dwyer, and Derek Smith for subtidal and intertidal collecting efforts in Washington. The following people and organizations kindly provided facilities access and related assistance: University of Washington Biology (and especially Ron Killman and Alex Hanson), Jim Truman, Lynn Riddiford, Merrill Hille, Rose Ann Cattolico, Evelyn Lessard, Mike Foy, Carolyn Friedman, Bryanda Wippel, Jacqueline Padilla-Gamiño, Jeremy Axworthy, Miranda Roethler, Julie Keister, the Port Townsend Marine Science Center, the Seattle Aquarium, Doug Engel, Tom Campbell, and Tommy Pieples. For conversations and other miscellaneous assistance, we thank Walter Heady, Rebecca Guenther, Jon Allen, Ryan Crim, Sophie George, Richard Strathmann, Mike Barker, Mary Sewell, Donald Greer, David Cohen, Kathy Foltz, Aidan Cox, Beatriz Velazquez, Chloe Deodato, Mo Turner, Wai-Pang Chan, Drew Harvell, Morgan Eisenlord, Megan Dethier, Julia Kobelt, and Aaron Galloway. Nyle Taylor at Taylor Shellfish and Ryan Crim at the Puget Sound Restoration Fund delivered juvenile bivalves at a moment's notice. Rebecca Guenther, Matt Ferner, Richard Strathmann, and two anonymous reviewers kindly provided comments on an earlier draft. Brady Blake and the Washington Department of Fish and Wildlife approved transfer permits, allowing us to move our operation between Friday Harbor and Seattle. Generous funding came from the Nature Conservancy (to JH) and California SeaGrant (NA18OAR4170073 to B. Gaylord, M. Baskett, A. Ricart, M. Edwards, M. Zippay, B. Hughes, S. Place, and JH). We dedicate this paper to John Pearse, who in one of his last conversations with JH asked, "Do you think you can figure out the juvenile rearing problem?" We're getting there, John!

Data Accessibility

Upon publication, primary data will be publicly accessible at the following link in the ResearchWorks archive at the University of Washington: http://hdl.handle.net/1773/46681.

Literature Cited

Adams, N. L., A. Heyland, L. L. Rice, and K. R. Foltz. 2019. Procuring animals and culturing of eggs and embryos. *Methods Cell Biol.* **150:** 3–46.

Allen, J. D., A. M. Reitzel, and W. Jaeckle. 2018. Asexual reproduction of marine invertebrate embryos and larvae. Pp. 271–276 in *Evolutionary Ecology of Marine Invertebrate Larvae*, T. J. Carrier, A. M. Reitzel, and A. Heyland, eds. Oxford University Press, New York.

Barker, M. F. 1978. Structure of the organs of attachment of brachiolaria larvae of *Stichaster australis* (Verrill) and *Coscinasterias calamaria* (Gray) (Echinodermata: Asteroidea). *J. Exp. Mar. Biol. Ecol.* **33:** 1–36.

Barker, M. F. 1979. Breeding and recruitment in a population of the New Zealand starfish *Stichaster australis* (Verrill). *J. Exp. Mar. Biol. Ecol.* **41:** 195–211.

Bates, D., M. Maechler, B. Bolker, and S. Walker. 2015. Fitting linear mixed-effects models using lme4. *J. Stat. Softw.* **67:** 1–48.

Burt, J. M., M. T. Tinker, D. K. Okamoto, K. W. Demes, K. Holmes, and A. K. Salomon. 2018. Sudden collapse of a mesopredator reveals its complementary role in mediating rocky reef regime shifts. *Proc. R. Soc. B Biol. Sci.* **285:** 20180553.

Chia, F. S., and C. W. Walker. 1991. Echinodermata: Asteroidea. Pp. 301–353 in *Reproduction of Marine Invertebrates*, Vol. VI, *Echinoderms and Lophophorates*, A. C. Giese, J. S. Pearse, and V. B. Pearse, eds. Boxwood Press, Pacific Grove, CA.

~~**Cole, R. N., and W. W. Burggren. 1981.** The contribution of respiratory papulae and tube feet to oxygen uptake in the sea star *Asterias forbesi* (Desor). *Mar. Biol. Lett.* **2:** 279–287.~~ q17

Dayton, P. K. 1975. Experimental evaluation of ecological dominance in a rocky intertidal algal community. *Ecol. Monogr.* **45:** 137–159.

Deaker, D. J., B. Mos, H.-A. Lin, C. Lawson, C. Budden, S. A. Dworjanyn, and M. Byrne. 2020. Diet flexibility and growth of the early herbivorous juvenile crown-of-thorns sea star, implications for its boom-bust population dynamics. *PLoS One* **15:** e0236142.

<-- add Byrne et al. ref here (see below)

Byrne, M., B. Mirchin, M. Clements and D. J. Deaker. 2021. The waiting stage, prolonged residency in nursery habitats by juveniles of the predatory sea star Marthasterias glacialis. Biol. Bull. THIS ISSUE.

Denny, M. W., E. K. Nelson, and K. S. Mead. 2002. Revised estimates of the effects of turbulence on fertilization in the purple sea urchin, *Strongylocentrotus purpuratus*. *Biol. Bull.* **203:** 275–277.

Done, T. J. 1992. Phase shifts in coral reef communities and their ecological significance. *Hydrobiologia* **247:** 121–132.

Duggins, D. O. 1983. Starfish predation and the creation of mosaic patterns in a kelp-dominated community. *Ecology* **64:** 1610–1619.

Emlet, R. B., L. R. McEdward, and R. R. Strathmann. 1987. Echinoderm larval ecology viewed from the egg. Pp. 55–136 in *Echinoderm Studies*, Vol. 2, M. Jangoux and J. M. Lawrence, eds. Balkema, Rotterdam.

Feder, H. M. 1980. Asteroidea: the sea stars. Pp. 117–135 in *Intertidal Invertebrates of California*, R. H. Morris, D. L. Abbott, and E. C. Haderlie, eds. Stanford University Press, Palo Alto, CA.

Finger, D. J. I., M. L. McPherson, H. F. Houskeeper, and R. M. Kudela. 2021. Mapping bull kelp canopy in northern California using Landsat to enable long-term monitoring. *Remote Sens. Environ.* **254:** 112243.

Freeman, A. 2005. Size-dependent trait-mediated indirect interactions among sea urchin herbivores. *Behav. Ecol.* **17:** 182–187.

Gravem, S. A., W. N. Heady, V. R. Saccomanno, K. F. Alvstad, A. L. M. Gehman, T. N. Frierson, and S. L. Hamilton. 2020. *Pycnopodia helianthoides*. [Online]. IUCN Red List of Threatened Species 2020, e.T178290276A178341498. Available: https://doi.org/10.2305/IUCN.UK.2020-3.RLTS.T178290276A178341498.en [2021, February 4].

Greer, D. L. 1962. Studies on the embryology of *Pycnopodia helianthoides* (Brandt) Stimpson. *Pac. Sci.* **16:** 280–285.

Haesaerts, D., M. Jangoux, and P. Flammang. 2005. The attachment complex of brachiolaria larvae of the sea star *Asterias rubens* (Echinodermata): an ultrastructural and immunocytochemical study. *Zoomorphology* **124:** 67–78.

Harvell, C. D., D. Montecino-Latorre, J. M. Caldwell, J. M. Burt, K. Bosley, A. Keller, S. F. Heron, A. K. Salomon, L. Lee, O. Pontier *et al.* 2019. Disease epidemic and a marine heat wave are associated with the continental-scale collapse of a pivotal predator (*Pycnopodia helianthoides*). *Sci. Adv.* **5:** eaau7042.

Hodin, J., M. C. Ferner, A. Heyland, and B. Gaylord. 2018. I feel that! Fluid dynamics and sensory aspects of larval settlement across scales. Pp. 190–207 in *Evolutionary Ecology of Marine Invertebrate Larvae*, T. J. Carrier, A. M. Reitzel, and A. Heyland, eds. Oxford University Press, New York.

Hodin, J., A. Heyland, A. Mercier, B. Pernet, D. L. Cohen, J.-F. Hamel, J. D. Allen, J. S. McAlister, M. Byrne, P. Cisternas *et al.* 2019. Culturing echinoderm larvae through metamorphosis. *Methods Cell Biol.* **150:** 125–169.

Hodin, J., M. C. Ferner, and B. Gaylord. 2020. Choosing the right home: Settlement responses by larvae of six sea urchin species align with hydrodynamic traits of their contrasting adult habitats. *Zool. J. Linn. Soc.* **190:** 737–756.

IUCN (International Union for Conservation of Nature). 2020. The IUCN Red List of Threatened Species. Version 2020-3. [Online]. Available: https://www.iucnredlist.org [2021, February 4].

Karp-Boss, L., E. Boss, and P. A. Jumars. 1996. Nutrient fluxes to planktonic osmotrophs in the presence of fluid motion. *Oceanogr. Mar. Biol. Annu. Rev.* **34:** 71–107.

Kenyon, K. W. 1969. The sea otter in the eastern Pacific Ocean. *N. Am. Fauna* **68:** 1–352.

Lefkovitch, L. P. 1965. The study of population growth in organisms grouped by stages. *Biometrics* **21:** 1–18.

Lenth, R. 2018. emmeans: estimated marginal means, aka least-squares means. [Online]. R package version 1.1.2. Available: https://CRAN.R-project.org/package=emmeans [2021, September 8]. **q18**

Margolin, A. S. 1976. Swimming of the sea cucumber *Parastichopus californicus* (Stimpson) in response to sea stars. *Ophelia* **15:** 105–114.

Metaxas, A. 2013. Larval ecology, settlement, and recruitment of Asteroids. Pp. 59–66 in *Starfish: Biology and Ecology of the Asteroidea*, J. M. Lawrence, ed. Johns Hopkins University Press, Baltimore.

Martinez, A. S., M. Byrne, and R. A. Coleman. 2017. Filling in the grazing puzzle: a synthesis of herbivory in starfish. Pp. 1–34 in *Oceanography and Marine Biology: An Annual Review*, Vol. 55, S. J. Hawkins, A. J. Evans, A. C. Dale, L. B. Firth, D. J. Hughes, and I. P. Smith, eds. CRC Press/Taylor & Francis, Boca Raton, FL.

Mauzey, K. P., C. Birkeland, and P. K. Dayton. 1968. Feeding behavior of asteroids and escape responses of their prey in the Puget Sound region. *Ecology* **49:** 603–619.

McEdward, L. R., and B. G. Miner. 2001. Larval and life-cycle patterns in echinoderms. *Can. J. Zool.* **79:** 1125–1170.

Moitoza, D. J., and D. W. Phillips. 1979. Prey defense, predator preference, and nonrandom diet: the interactions between *Pycnopodia helianthoides* and two species of sea urchins. *Mar. Biol.* **53:** 299–304.

Murphy, C. T., and M. B. Jones. 1987. Some factors affecting the respiration of intertidal *Asterina gibbosa* (Echinodermata: Asteroidea). *J. Mar. Biol. Assoc. U.K.* **67:** 717–727. **q19**

Nishizaki, M. T., and J. D. Ackerman. 2007. Juvenile-adult associations in sea urchins (*Strongylocentrotus franciscanus* and *S. droebachiensis*): protection from predation and hydrodynamics in *S. franciscanus*. *Mar. Biol.* **151:** 135–145.

R Core Team. 2017. R: a language and environment for statistical computing. [Online]. R Foundation for Statistical Computing, Vienna. Available: https://www.R-project.org/ [2021, September 8]. **q20**

Rogers-Bennett, L., and C. A. Catton. 2019. Marine heat wave and multiple stressors tip bull kelp forest to sea urchin barrens. *Sci. Rep.* **9:** 15050.

Shivji, M., D. Parker, B. Hartwick, and M. J. Smith. 1983. Feeding and distribution study of the sunflower sea star *Pycnopodia helianthoides* (Brandt, 1835). *Pac. Sci.* **37:** 133–140.

Sloan, N. A. 1980. Aspects of the feeding biology of asteroids. *Oceanogr. Mar. Biol. Annu. Rev.* **18:** 57–124.

Strathmann, M. F. 1987. *Reproduction and Development of Marine Invertebrates of the Northern Pacific Coast*. University of Washington Press, Seattle.

Strathmann, R. R. 2014. Culturing larvae of marine invertebrates. Pp. 1–25 in *Methods in Molecular Biology*, Vol. 1128, *Developmental Biology of the Sea Urchin and Other Marine Invertebrates, Methods and Protocols*, D. J. Carroll and S. A. Stricker, eds. Springer, New York.

Taylor, G. I. 1923. Stability of a viscous liquid contained between two rotating cylinders. *Philos. Trans. R. Soc. A Math. Phys. Eng. Sci.* **232:** 289–343.

DATA SUPPLEMENT for

Progress towards complete life-cycle culturing of the endangered sunflower star *Pycnopodia helianthoides*

Hodin J, Pearson-Lund A, Anteau FP, Kitaeff P and S Cefalu

The Biological Bulletin, Dec 2021, volume 241, number 3. https://doi.org/10.1086/716552

SUPPLEMENTARY MATERIALS & METHODS

1. Collecting, feeding, holding and distinguishing adults

In addition to the stars collected in 2019 as described in the main text, we also received documentation during this period of sighting of three additional sunflower stars > 20 cm that were not collected. Our chosen collection locales were made up of sites that *P. helianthoides* had historically been observed pre-SSW, as well as some additional sites. We found that certain locations (such as subtidal areas around Reuben Tarte County Park; 48.612 N, 123.097 W) represented apparent 'hot spots' where we had repeated success finding individuals of a range of sizes (including several <20 cm diameter that we did not collect), whereas other locations with formerly (pre-2013) robust populations (such as Point Caution; 48.563 N, 123.017 W) yielded zero observed individuals despite our repeated collecting attempts. All told, these collections and sightings of 38 total stars in 6 mo required 84 person-hours of searching (i.e., ~2.2 person-hours for each >20 cm sunflower star found). Note that our searches became more successful towards the end of this collecting period, as we focused our searches in 'hot spot' locales.

Adult *P. helianthoides* maintained in the same aquaria are gregarious (remaining in contact with one another for long periods despite room to separate) and only display aggressive interactions during feeding. During Spring 2019, a few of the captive adults exhibited signs of SSW, including arm curling behavior and arm autotomy. These animals and all of their aquarium mates (5 stars total) were then returned to the field where we hoped that they would have a better chance of recovery. From June 2019 until June 2021 (the time of this writing), we have maintained 28 of 30 stars continually with no further instances of wasting symptoms observed. The 29th star was found dead in Nov 2020 on the ground near one of our tanks; we suspect it was a victim of a raccoon (*Procyon lotor*) predation event. The 30th star was released due to poor apparent condition in Spring 2021, at its site of collection 2 years earlier: the dock pilings at Friday Harbor Labs. In subsequent weeks, we encountered this star several times at a similar location, confirming that he had survived reintroduction and his condition had improved. His color pattern and the position of his amputated arms allowed us to know for certainty that this was the same star that we had released. For more on our methods for identifying individual stars, see Supplementary Figure S1 (below).

2. Assessing reproductive status, obtaining gametes, maturation and fertilization

We prepared 1-MA stock solutions by first making a 2.5% solution of 1-MA (Fisher Scientific Acros 201310250) in dimethyl sulfoxide (DMSO). We then diluted that 1:1130 in 1 µm-filtered seawater (henceforth MFSW) to make a 100 µM 1-MA stock solution (final DMSO concentration: <0.1%), which we sterile-filtered through a 0.2 µm syringe filter and stored at 4°C.

We attempted 1-MA injections to induce spawnings on 15 different occassions over 24 months, and we were only successful three times: May 2019 (only 1 male spawned); Sept 2019 (only one male spawned) and April 2021 (3 males and 1 female spawned, with the female releasing few total eggs, but they did fertilize; see Table 1 in main text). At 11-12°C, these five males began spawning between 55 and 110 min after injection; the one female began spawning 155 min after injection.

We attempted a aboral flap incisions of epidermis in three stars [Assessment Method (2); see the main text]. While this method did allow us easy access to sample the gonad, recovery from incision was poor: all three of these stars autotomized the adjacent arm within 2 d of dissection. We then released those stars due to SSW concerns, allowing them to recover in the wild. Note that the poor recovery from incision has been previously reported in the ochre sea star, *Pisaster ochraceous* (Sanford et al. 2009), so we do not recommend this technique.

By contrast, and consistent with the aforementioned findings of Sanford and colleagues (2009) for *P. ochraceous*, arm amputation is an effective gonad sampling method in *P. helianthoides*, and results in excellent recovery. In the 16 mo between Sep 2019 and Jan 2021, we amputated an arm in 22 of the stars; all have recovered, the amputated arms are all regenerating (see Supplemental Results, below), and none of these stars has subsequently exhibited signs of wasting. Furthermore, 12 of these 22 stars have received two amputations (with amputations separated by at least 6 mo), again with no observed ill effects.

Finally, we note that if an adult star were to self-autotomize an arm, as often occurs during advanced stages of SSW, it is often possible to recover gonad for analysis. It is worth noting that stars that succumb to wasting would probably not be an appropriate choice for siring offspring for captive breeding programs, though it could be of research interest (e.g., in studying potential parent-offspring transmission). Sampling gonad in wasting stars could provide valuable information on reproductive seasonality, so we recommend doing so with appropriate precautions. Dissecting tools, dishes and other laboratory implements that come into contact with tissue from adults showing signs of wasting should be thoroughly decontaminated before use with healthy individuals or their gonadal tissues.

The viability of male gonadal tissue can be assessed by making a slide preparation in sea water and examining it under 100x or greater power. Mature, viable male gonad should contain highly active sperm. Female gonadal tissue can be assessed similarly, but in this case the cover glass should be raised slightly (with, e.g., clay "feet"; see Strathmann 2014) so that the oocytes remain uncompressed, allowing their diameters to be accurately measured to assess maturity. We measured oocyte diameters by one of two methods: (1) with a calibrated ocular micrometer; or (2) from micrographs with known pixel calibration.

If oocytes are obtained by natural or induced spawning from intact females, what will be recovered should be mainly fully mature oocytes (see Fig. 2B in the main text) which should then complete meiosis and germinal vesicle breakdown (GVBD) in situ over the following 60 min or more, at which point they are fertilizable (Strathmann 1987; Adams et al. 2019; see Fig. 2 in the main text). If mature oocytes are recovered by dissection [methods (2-4) above], then the pieces of dissected ovary must be treated with 1 µM 1-MA in MFSW for >60 min for them to release ("spawn") oocytes and then complete meiosis and GVBD (see Fig. 2A-C, in the main text).

Oocytes having undergone GVBD (Figure 2C in the main text) are fertilizable for the subsequent ~24 h or even more, using a freshly diluted sperm suspension, but the highest proportion of fertilized eggs occurs in the first 6 h after GVBD. We conducted all fertilizations at 10-11°C in 100 ml beakers by adding 10-20 drops of a fresh, dilute sperm suspension (approximately 1:300) in MFSW, and then stirring the water in the beakers for 5 sec. After eggs settled, we decanted off the sperm-filled water, and replaced with fresh MFSW. *P. helianthoides* eggs have clearly visible fertilization membranes, raised approximately 10 µm from the egg surface (see Fig. 2D in the main text). See Strathmann (1987) and Adams et al. (2019) for more detailed methods.

3. Embryogenesis and larval development

No supplemental notes.

4. Settlement and completion of metamorphosis

We define metamorphosis as a major morphological transformation from one life history stage to a subsequent one, often involving a change in habitat (Hodin 2006; for other definitions see Bishop et al. 2006). In echinoderms, this transformation involves a radical change in symmetry from what is generally a bilaterally-symmetric planktonic larval form into a pentameral juvenile in the benthos. Still, in many echinoderms (including *P. helianthoides*), the shift from bilateral to pentameral begins within the feeding larval body itself. Therefore, we consider metamorphosis in *P. helianthoides* to begin at approximately 27 dpf, when juvenile-structures structures appear in the rudiment and to end a few days after the transition to the sea floor, at which point the benthic juvenile can feed. Inherent in this conception is that the irreversible habitat shift from the plankton to the benthos – namely, *settlement*– is a key stage in the metamorphic process, but is not *sensu stricto* synonymous with metamorphosis. In summary, metamorphosis is the morphological change from larva to juvenile; settlement is the shift in habitat.

The Taylor-Couette cell that we used consisted of two concentrically nested cylinders separated by a 3.5 mm gap filled with seawater, into which we introduced larvae by gently pouring from their selection beaker through a funnel. Relative rotation of the two cylinders sheared the water in the gap between the cylinders, and did so strongly enough to generate turbulent flow. Turbulence generated by the Taylor–Couette cell recreates many of the features of natural turbulence produced beneath breaking waves, where kinetic energy is translated down through ever-smaller eddies to the smallest scales of fluid motion until that turbulent energy is dissipated by viscosity. More intense turbulence results in higher levels of energy dissipation, indexed in watts per kilogram (= m^2 s^{-3}), and a broader energy cascade that sustains eddies of tinier size, smaller than (hence detectable by) marine larvae.

The Couette device we used here is identical to one used in prior publications focused on echinoid larvae (see Hodin et al. 2020 and references therein), and we here tested a single turbulence intensity of ~5 W kg^{-1} (which at 11°C in our device corresponds to a rotation rate of 500 rpm). We selected this level of exposure based on peak intensities of turbulence that have been measured in the field on exposed rocky shores in the NE Pacific (a historical habitat for some P. helianthoides populations), and which also elicited responses across echinoid taxa in previous studies (Gaylord 2008; Gaylord et al. 2013; Hodin et al. 2015; Hodin et al. 2020).

5. Culturing juveniles post-settlement

In our initial efforts to culture the post settlement stages, the cultures experienced high mortality. We attribute this mortality to a combination of the following causes:

a. **Physical damage**. As mentioned previously, the juveniles tend to adhere extremely strongly during the settlement process and are quite resistant to dislodgement. Using, for example, a high intensity water stream will ultimately dislodge them, but often results in tissue damage to the juvenile. We suspect that damaged juveniles subsequently exhibit poor survival.

b. **Contaminants**. Due to the location of our initial juvenile culturing efforts, we did not have access to flowing sea water, so we used recirculating natural sea water tanks, with seawater water filtered to a nominal 20 µm. This resulted in the rapid accumulation of ciliates, benthic diatom fouling and other microbial contaminants that were associated with mortality of juveniles. Once such contaminants enter the cultures, they are exceedingly difficult to remove. Even transferring individual juveniles out of contaminated containers into fresh ones can result in incidental transfer of contaminants, which will then infect the new container. We subsequently increased our filtration level down to a nominal 1 µm ("MFSW"), which likely decreased upstream sources of new contaminants. We did not have access to UV treatment except in one set of experiments with Alaskan stars. We recommend employing UV treatment if available to limit upstream contamination, while noting that it is possible that a certain complement of microbes might be beneficial to juvenile development.

c. **Closed culture**. Whereas the small jars we described previously were useful for settlement experiments, post-settlement observations and transport of cultures, juveniles maintained under these conditions eventually experienced high mortality, despite frequent (every other day) water exchanges. We attribute this high mortality to a combination of causes, including the aforementioned contaminants, low oxygen levels, especially in the biofilm boundary layer, and, finally, a positive feedback of juvenile deaths resulting in culture fouling, an increase in contaminant populations, and further death.

d. **Cannibalism**. In the absence of an alternate food source, the juveniles will readily resort to cannibalism, thus resulting in another significant source of mortality. Especially during our initial rearing efforts, during which time we had not identified a quality food source for the young juveniles, we directly observed several instances of cannibalism, and inferred others from the disappearance of juveniles between observations. See also Brocco French and Allen (2021).

6. Transport of different life stages

Gametes. Sperm collected 'dry' and dissected pieces of testis can be transported on ice, and stored for one week or longer in capped tubes at 4°C and remain viable. Pieces of dissected ovary (untreated with 1-MA) can be stored for at least 2 d at cold ambient temperatures (~8-10°C) in MFSW and remain viable. For transport of dissected ovary pieces, we placed them inside 125-250 ml tissue culture flasks, filled to the brim with MFSW, the tops sealed with parafilm (ideally with no air bubble), and then reinforced with plastic wrap (i.e., cling film), affixed tightly to the flask neck with a rubber band, and kept cool during transport between two 4°C-equilibrated ice packs inside a polystyrene cooler.

Larvae. We transported larvae successfully over a 12-h period in the manner described above for ovary pieces, except that we used larger flasks and maintained the larvae no more than 3x their current culturing density. We did not attempt longer transport, but based on our success in doing so as described with a variety of other echinoderm larvae (see, e.g., Hodin et al. 2020), including asteroids, we suspect that even a 1-2 d transport period by this method would be successful. For longer transport periods, larval density is ideally maintained at or near the current culturing density.

Juveniles. We successfully transported juveniles over a 12-h period by two different methods: in canning jars with plastic leak-proof lids (Ball), or in their culturing cages filled to 50% capacity inside outer plastic containers. In both cases, we placed the containers in coolers with 4°C-equilibrated ice packs.

Adults. In our experience, adult *Pycnopodia* do not tolerate long periods of transport (>1h) in still water (e.g., large coolers with sea water). We are aware of two occasions in which adults that were transported over longer time periods from their collection to their holding locales then subsequently succumbed to sea star wasting (SSW). In holding, adults survive best in constantly-flowing, well-oxygenated seawater. It is possible that if one could mimic these conditions during transport, then they might tolerate longer transport periods.

SUPPLEMENTARY RESULTS

Table S1. *P. helianthoides* oocyte sizes in Washington, 2019-2021, plus one observation from Alaska 2019. Abbreviations: 1-methyladenine, 1-MA; germinal vesicle breakdown, GVBD; oocytes with germinal vesicles, GV+, oocytes following GVBD, GV-; fertilized eggs, +FE (*N.b.*, measured zygote diameter, not including FE).; seastar wasting (SSW).

Sample number	Date, location and depth collected	Date oocytes measured	Description	Mean oocyte diameter	95% c.i.
1	Mar 2019, Friday Harbor WA, from FHL dock piling by hand	May 2019	Ovary sampled by dissection, oocytes did not undergo GVBD in response to 1-MA, measured GV+.	56.1	± 3.3
2	Jul 2019, Auke Bay, Juneau AK, subtidal 9 m	Jul 2019	Ovary recovered by arm amputation, shipped to Friday Harbor, matured in 1-MA, oocytes fertilized, measured +FE.	165.3	± 2.7
3	Jul 2019, arm autotomized during attempted intertidal collection, Beaverton Cove, Friday Harbor WA	Jul 2019	Gonad completely devoid of oocytes (recently spawned?).	n/a	n/a
4	Jun 2019, Cattle Point, San Juan Island WA, intertidal by hand	Sep 2019	Ovary recovered by arm amputation, oocytes did not undergo GVBD in response to 1-MA, measured GV+.	77.6	± 6.3
5	Jun 2019, off Brown Island, Friday Harbor WA, subtidal 12 m	Sep 2019	As above.	50.3	± 8.8
6	Jun 2019, near FHL dock, Friday Harbor WA, subtidal 12 m	Nov 2019	Ovary recovered by arm amputation, ovary treated with 1-MA, measured GV- subset with +FE following sperm addition.	164	± 2.2

7	As above (Sample 6)	Nov 2019	As above, here measured subset of oocytes that did not undergo GVBD (GV+).	139.5	± 9.9
8	Jul 2019, Snug Harbor, San Juan Island WA, subtidal 10 m	Nov 2019	Ovary recovered by arm amputation, ovary treated with 1-MA, measured +FE.	157.8	± 3.6
9	Aug 2019, O'Neill Island (off San Juan Island) WA, subtidal 13 m	Nov 2019	Ovary recovered by arm amputation, ovary treated with 1-MA, did not undergo GVBD, measured GV+.	95.4	± 5.8
10	Aug 2019, off Brown Island, Friday Harbor WA, subtidal, in crab pot, unknown depth	Nov 2019	As above.	101.3	± 5.8
11	Jan 2020, Sund Rock, Hood Canal WA, subtidal 9-15 m	Jan 2020	Ovary recovered from arm dropped following SSW. Not treated with 1-MA; measured GV+.	157	± 4.7
12	Jan 2020, Sund Rock, Hood Canal WA, subtidal 9-15 m	Feb 2020	As above.	167.1	± 6.6
13	July 2019, near FHL dock, Friday Harbor WA, subtidal 8 m	Apr 2020	Ovary recovered by arm amputation, ovary treated with 1-MA, measured GV-.	168.2	± 2.9
14	June 2019, Snug Harbor, San Juan Island WA, intertidal by hand	Apr 2020	As above.	155.8	± 4.8
15	Aug 2020, Goose Island (Cattle Pass) WA, subtidal 10 m	Sep 2020	Ovary recovered from arm dropped following SSW. Not treated with 1-MA; measured GV+.	83.2	± 5.9
16	June 2019, Snug Harbor, San Juan Island WA, intertidal by hand (*same star as in Sample 14*)	Nov 2020	Ovary recovered by arm amputation, ovary treated with 1-MA, some oocytes appeared to undergo GVBD, measured GV-. No oocytes successfully fertilized.	126.2	± 4.1

17	July 2019, near FHL dock, Friday Harbor WA, subtidal 8 m (*same star as in Sample 13*)	Nov 2020	As above.	130.3	± 4.7
18	Aug 2019, O'Neal Island (off San Juan Island) WA, subtidal 13 m (*same star as in Sample 9*)	Nov 2020	As above.	137.9	± 5.6
19	Aug 2019, off Brown Island, Friday Harbor WA, subtidal, in crab pot, unknown depth. (*same star as in Sample 10*)	Jan 2021	Ovary recovered by arm amputation, treated with 1-MA, underwent GVBD, and successfully fertilized. Measured GV+ before 1-MA addition.	159.9	± 5.2
20	Jun 2019, Cattle Point, San Juan Island WA, intertidal by hand (*same star as in Sample 4*)	Jan 2021	As above.	166.9	± 6.3

Supplementary Figures and Explanatory Text

Adult Identification

Figure S1 provides a guide for how to identify and track individual stars. Although the color patterns have been quite consistent in the vast majority of our captive stars over time (Fig. S1E, F), there are subtle exceptions (Fig. S1C, D).

Juvenile survival and growth

As seen in Fig. 10 (see main text) and Figs S3 and S4 (below), we had increasing success with juvenile survival and growth once juveniles reached approximately 1 mm, at which point they began to consume juvenile bivalves. Initially, we crushed individual bivalves to give the sea star juveniles access to the flesh; older sea star juveniles began to open and consume live bivalves. **Figure S2** shows the relationship between *P. helianthoides* juvenile diameter and volume of juvenile bivalves (crushed or intact) consumed per day.

Figure S3 shows juvenile survival over time, with each line representing numbers of surviving juveniles within an independent growth chamber. The clear trend is high attrition early in juvenile ontogeny with greater survival after a few months. We are unable to evaluate the extent to which this pattern is a function of normal attrition in the early juvenile stage of *P. helianthoides* as opposed to our aforementioned explorations into different growth conditions.

Figure S4 shows juvenile growth over time, in this case with each line representing a single individual. Note that in only a subset of cases were we able to definitively identify individuals within a vessel in repeated measures –for example, by their numbers of arms or other distinguishing features. In most of the data shown here, we assumed for the purpose of this analysis that individual juveniles sharing a culture vessel maintained their relative rank order of sizes. As in the aforementioned survival data, the overall pattern here is slow initial growth with rapid increases in growth rates at larger sizes. And again, we are here unable to evaluate the extent to which this pattern is a reflection of our offering quality food sources only to the larger individuals rather than it being a normal ontogenetic pattern for the species.

Figure S1

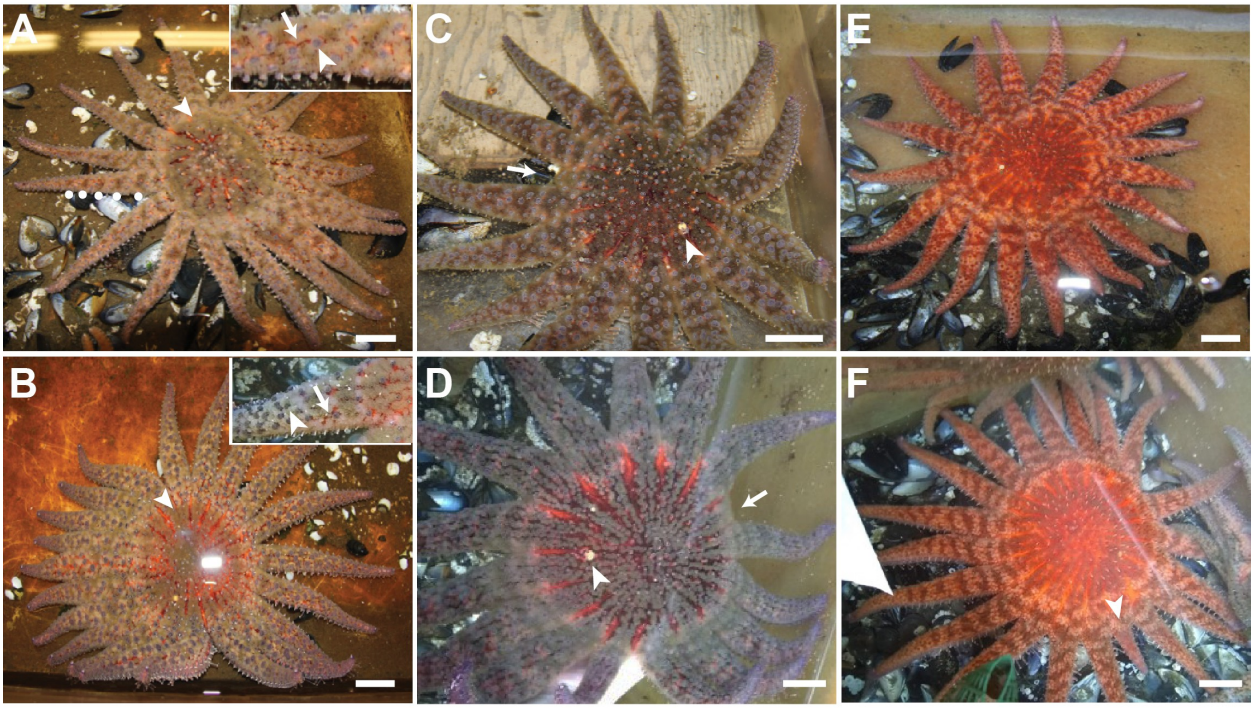

Figure S1. Individual identification in *P. helianthoides*, exemplified in four of our captive stars. Contrasting two stars in (A) and (B). The star in A is more silver overall, is greener and fuzzier around the central disk [this is presumably from respiratory papulae (Cole & Burggren 1981); compare *white arrowheads* in main panels of A, B], and has a disorganized stripe pattern down each arm (marked at left in A by *white dots*); the arms of the star in B are not striped. Also, the star in A has prominent blue spines; those of the star in B are prominent and brown (compare *white arrowheads* in the insets in A, B). Both stars share burgundy reticulations (*white arrows* in insets in A, B), a feature absent in most other stars. (C, D) Change in a third star's color over 18 mo. In late 2019 (C) this star had an overall plum color, prominent blue spines, disorganized plum arm stripes and purple arm tips. In early 2021 (D) these features were still present, but had become obscured by a silvery-green fuzzy appearance (papulae, which can be retracted; Murphy & Jones 1987) overlaying the arms and central disk. This star's diagnostic arm stub (*white arrows* in C, D), the only non-regenerating arm that we have observed in *P. helianthoides*, was present upon collection in mid 2019, and unchanged since. The stub is 7 arms clockwise from the madreporite (*white arrowhead* in C, D). (E, F) Consistent coloration and patterns in a fourth star from late 2019 (E) to late 2020 (F). Note the bright orange coloration and regular arm stripes in both E and F [c.f., the less well-organized arm stripes in A and C, D]. The *white arrowhead* in F indicates the regenerating arm, 11 mo after amputation. Scale bars are 5 cm.

Figure S2

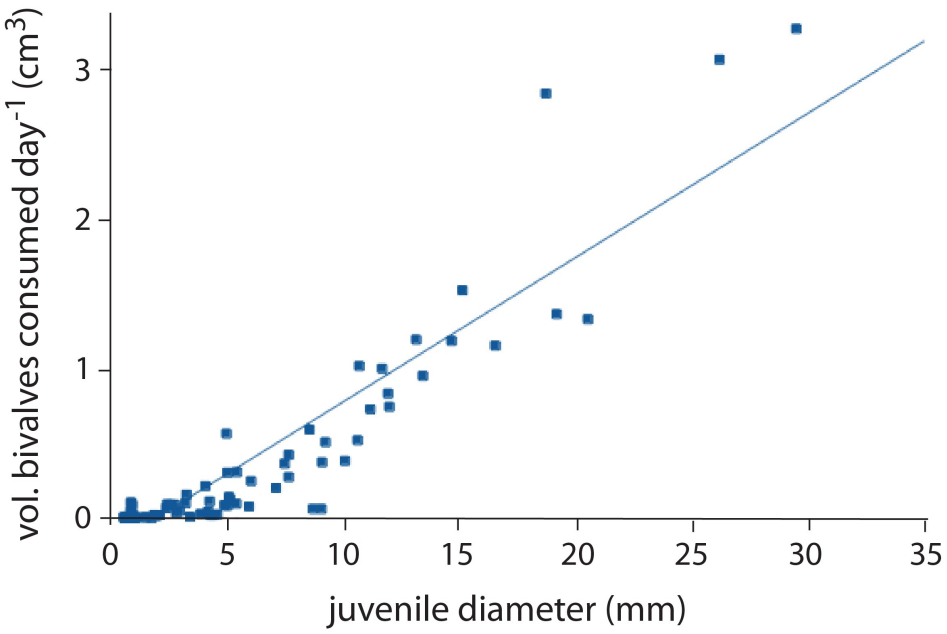

Figure S2. Juvenile feeding. Strong linear relationship (R^2=0.846) between juvenile size and volume of bivalves consumed each day. Our data on the largest juvenile stars (>2 cm diameter) is recent and thus limited, but might suggest an increased rate of consumption by body size later in juvenile ontogeny.

Figure S3

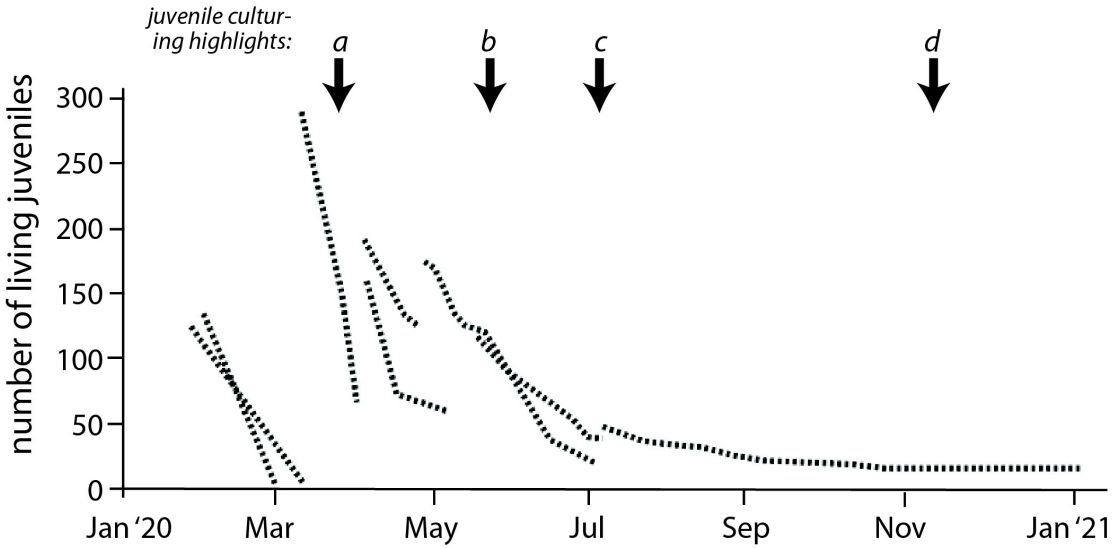

Figure S3. Juvenile mortality in WA stars in the first year after settlement. Each line represents an independent vessel or set of vessels cultured in a similar manner. When the lines end, the remaining juveniles were moved to new vessels, locations or culturing conditions. The general pattern is high mortality early, with increased survival rates over time (see also Fig. 10 in the main text). *Arrows* and *lowercase letters* at the top indicate dates at which we made significant changes to culturing conditions as follows. ***a***–juveniles moved from static to recirculating flow conditions. ***b***– began feeding juveniles crushed Manila clams and Pacific oysters. ***c***–juveniles separated by size in an effort to limit cannibalism. ***d***–juveniles moved into continuously flowing, micron-filtered sea water at FHL.

Figure S4

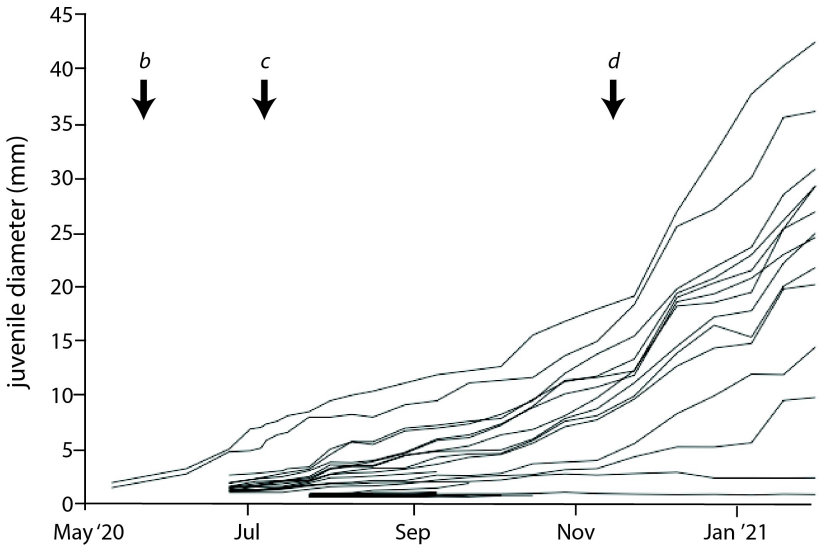

Figure S4. Juvenile growth in individual WA stars. Each line represents the growth trajectory of a single star from May 2020 until Jan 2021. Lines that end before Jan 2021 represent stars that died. Two trends from this graph are: (1) the high variation in growth rate among stars raised in similar conditions; and (2) growth rates generally appear to accelerate once stars reach approximately 10 mm in diameter. This is approximately the size at which juveniles are able to open and consume live juvenile bivalves; before that point, we crush the bivalve shells for the sea star juveniles. Note that for this analysis we made the simplifying assumption that individual stars within a cage maintain their relative rank order of sizes between measurements. *Lowercase letters above arrows* indicate changes in juvenile culturing conditions: ***b***– began feeding juveniles crushed Manila clams and Pacific oysters. ***c–***juveniles separated by size in an effort to limit cannibalism. ***d***–juveniles moved into continuously flowing, micron-filtered sea water at FHL.

SUPPLEMENTAL REFERENCES CITED

Adams, N. L., A. Heyland, L. L. Rice and K. R. Foltz. **2019**. Procuring animals and culturing of eggs and embryos. Pp 3–46 in *Methods in Cell Biology*, K. R Foltz and A. Hamdoun, eds. *Echinoderms – Part A*. **150**. Chapter 1. Elsevier, New York.

Bishop, C. D., D. F. Erezyilmaz, T. Flatt, C. D. Georgiou, M. G. Hadfield, A. Heyland, J. Hodin, M. W. Jacobs, S. A. Maslakova, A. Pires, *et al.* 2006. What is metamorphosis? *Integrative and Comparative Biology* **46**: 655–661.

Brocco French, K. I. and J. D. Allen. 2021. Cannibalism of newly metamorphosed juvenile sea stars. *Ecology* doi:10.1002/ecy.3352

Cole, R. N., and W. W. Burggren. 1981. The contribution of respiratory papulae and tube feet to oxygen uptake in the sea star *Asterias forbesi* (Desor). *Mar. Biol. Lett.* **2**: 279–287.

Gaylord, B. 2008. Hydrodynamic context for considering turbulence impacts on external fertilization. *The Biological Bulletin* **214**: 315–318.

Gaylord, B., J. Hodin and M. C. Ferner. **2013**. Turbulent shear spurs settlement in larval sea urchins. *Proceedings of the National Academy of Sciences, USA* **110**: 6901–6906.

Hodin, J. 2006. Expanding networks: Signaling components in and a hypothesis for the evolution of metamorphosis. *Integrative and Comparative Biology* **46**: 719–742.

Hodin, J., M. C. Ferner, G. Ng, C. J. Lowe and B. Gaylord. **2015**. Rethinking competence in marine life cycles: ontogenetic changes in the settlement response of sand dollar larvae exposed to turbulence. *Royal Society Open Science* **2**: 150114.

Hodin J., M. C. Ferner and B. Gaylord. **2020**. Choosing the right home: settlement responses by larvae of six sea urchin species align with hydrodynamic traits of their contrasting adult habitats. *Zoological Journal of the Linnean Society* **190**: 737–756.

Murphy, C. T., and M. B. Jones. 1987. Some factors affecting the respiration of intertidal *Asterina gibbosa* (Echinodermata: Asteroidea). *J. Mar. Biol. Assoc. U.K.* **67**: 717–727.

Sanford, E., M. E. Wood and K. J. Nielsen. **2009**. A non-lethal method for estimation of gonad and pyloric caecum indices in sea stars. *Invertebrate Biology* **128**: 372–380.

Strathmann, M. F. 1987. *Reproduction and Development of Marine Invertebrates of the Northern Pacific Coast*. University of Washington Press: Seattle.